Supporting Information, Organometallics, 2012.

Blue Phosphorescence of Trifluoromethyl- and Trifluoromethoxy-Substituted Cationic Iridium(III) Isocyanide Complexes

Nail M. Shavaleev,*[,a] Filippo Monti,[b] Rosario Scopelliti,[a] Nicola Armaroli,*[,b] Michael Grätzel,[a] Mohammad K. Nazeeruddin*[,a]

[a]Laboratory of Photonics and Interfaces, École Polytechnique Fédérale de Lausanne, CH-1015 Lausanne, Switzerland
[b]Molecular Photoscience Group, Istituto per la Sintesi Organica e la Fotoreattività, Consiglio Nazionale delle Ricerche, Via P. Gobetti, 101, 40129, Bologna, Italy

*Corresponding authors.
Tel.: +41 21 693 6124; fax: +41 21 693 4111.
E-mail addresses: nail.shavaleev@epfl.ch; nicola.armaroli@cnr.it; mdkhaja.nazeeruddin@epfl.ch.

Contents

1. Synthesis of 2-Phenylpyridines

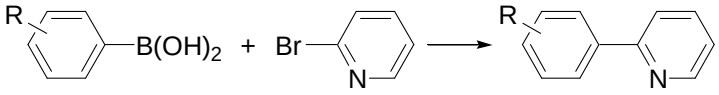

The reactions were performed under argon. The solvents were de-oxygenated by bubbling with Ar, but they were not dried. 2-Bromopyridine (Aldrich), arylboronic acid (excess), and K_2CO_3 (excess, Fluka) were dissolved in THF/water (30/10 mL) at RT, followed by addition of $Pd(PPh_3)_4$ (catalyst, Strem). The reaction mixture was stirred at 85 °C for 48 h (**L1**, **L3**–**L8**) or 72 h (**L2**) to give orange or red solution. The organic solvent was rotor-evaporated, and the residue was extracted with ether (**L1**) or hexane (**L2**–**L8** are well-soluble in hexane) and water. The organic layer was washed several times with saturated aqueous solution of Na_2CO_3 to remove boronic acid, and then washed with water. The organic layer was evaporated to give red residue that was purified by column chromatography. The main problem in the purification is the removal of 2-bromopyridine, which precedes the product fraction. In some cases, after chromatography the product still contained an unidentified impurity (observed by ^{1}H NMR) that probably originated from boronic acid. In order to remove this impurity, the product was sonicated in aq. sol. of Na_2CO_3, and extracted with hexane. The organic layer was extracted again with aq. sol. of Na_2CO_3, washed with water, and evaporated to give the pure product. The details are provided below.

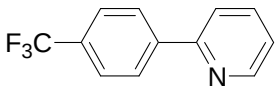

2-(4′-Trifluoromethylphenyl)pyridine, L1. The reaction was performed with 2-bromopyridine (0.51 mL, 0.84 g, 5.3 mmol), 4-trifluoromethylphenylboronic acid (1.13 g, 5.9 mmol, Aldrich), K_2CO_3 (1.8 g, 13 mmol), and $Pd(PPh_3)_4$ (77 mg, 0.067 mmol). Chromatography was run on silica (20 g) with hexane/CH_2Cl_2 (1/1) to remove impurities, and with hexane/CH_2Cl_2 (1/2) to recover the product. White crystalline solid: 1.12 g (5.0 mmol, 95%; $C_{12}H_8F_3N$; MW 223.19). ^{1}H NMR (400 MHz, DMSO-d_6): δ = 8.76–8.72 (m, 1H), 8.32 (d, J = 8.8 Hz, 2H), 8.12–8.07 (m, 1H), 7.96 (td, J = 7.6, 2.0 Hz, 1H), 7.87 (d, J = 8.8 Hz, 2H), 7.46 (ddd, J = 7.6, 4.8, 1.2 Hz, 1H) ppm. ^{13}C NMR (100 MHz, DMSO-d_6): δ = 155.03, 150.41, 143.09, 138.06, 129.89 (q, $J_{C–F}$ = 31 Hz), 127.84, 126.20 (q, $J_{C–F}$ = 3.6 Hz), 124.92 (q, $J_{C–F}$ = 269 Hz), 124.13, 121.53 ppm. ^{19}F NMR (376 MHz, DMSO-d_6): δ = −61.03 ppm. GC-EI$^+$ MS: m/z 223 (M^+, 60%), 154 ($\{M – CF_3\}^+$, 100%).

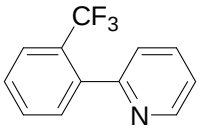

2-(2′-Trifluoromethylphenyl)pyridine, L2. The reaction was performed with 2-bromopyridine (0.42 mL, 0.69 g, 4.4 mmol), 2-(trifluoromethyl)benzeneboronic acid (1.1 g, 5.8 mmol, Aldrich), K_2CO_3 (1.87 g, 13.5 mmol), and $Pd(PPh_3)_4$ (87 mg, 0.075 mmol). Chromatography

was run on silica (15 g) with hexane/CH_2Cl_2 (2/1 to 1/1) to remove impurities, and with hexane/CH_2Cl_2 (1/3 to 1/4) to recover the product. Pale yellow oil: 970 mg (4.35 mmol, 99%; $C_{12}H_8F_3N$; MW 223.19). ^{1}H NMR (400 MHz, DMSO-d_6): δ = 8.69–8.62 (m, 1H), 7.92 (td, J = 7.6, 1.6 Hz, 1H), 7.87 (d, J = 8.0 Hz, 1H), 7.77 (t, J = 7.6 Hz, 1H), 7.68 (t, J = 7.6 Hz, 1H), 7.54 (d, J = 7.6 Hz, 1H), 7.50 (d, J = 7.6 Hz, 1H), 7.45 (ddd, J = 7.2, 4.8, 0.8 Hz, 1H) ppm. ^{13}C NMR (100 MHz, DMSO-d_6): 157.98, 149.59, 140.52 (q, $J_{C–F}$ = 1.9 Hz), 137.09, 132.83, 132.26, 129.36, 127.62 (q, $J_{C–F}$ = 30 Hz), 126.94 (q, $J_{C–F}$ = 4.9 Hz), 124.80 (q, $J_{C–F}$ = 272 Hz), 124.28 (q, $J_{C–F}$ = 1.9 Hz), 123.48 ppm. ^{19}F NMR (376 MHz, DMSO-d_6): δ = −55.40 ppm. GC-EI$^+$ MS: m/z 223 (M^+, 100%).

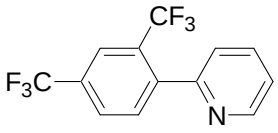

2-(2′,4′-Bis-(trifluoromethyl)phenyl)pyridine, L3. The reaction was performed with 2-bromopyridine (0.28 mL, 0.46 g, 2.9 mmol), 2,4-bis(trifluoromethyl)benzeneboronic acid (1 g, 3.9 mmol, Combi-Blocks Inc.), K_2CO_3 (1.24 g, 9.0 mmol), and $Pd(PPh_3)_4$ (114 mg, 0.099 mmol). Chromatography was run on silica (17 g) with hexane/CH_2Cl_2 (2/1 to 1/1) to remove impurities, and with hexane/CH_2Cl_2 (1/3) to recover the product. Colourless oil: 575 mg (1.97 mmol, 68%; $C_{13}H_7F_6N$; MW 291.19). It is difficult to separate **L3** from 2-bromopyridine by chromatography; therefore, it is recommended to run the reaction with an excess of the boronic acid, higher amount of catalyst, and for a longer time in order to completely convert 2-bromopyridine to **L3**. ^{1}H NMR (400 MHz, DMSO-d_6): δ = 8.73–8.68 (m, 1H), 8.22–8.16 (m, 2H), 7.97 (td, J = 8.0, 2.0 Hz, 1H), 7.82 (d, J = 8.4 Hz, 1H), 7.59 (d, J = 8.0 Hz, 1H), 7.51 (ddd, J = 8.0, 4.8, 1.2 Hz, 1H) ppm. ^{19}F NMR (376 MHz, DMSO-d_6): δ = −55.90 (3F), −61.29 (3F) ppm. GC-EI$^+$ MS: m/z 291 (M^+, 100%).

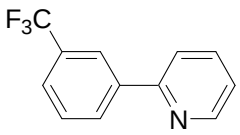

2-(3′-Trifluoromethylphenyl)pyridine, L4. The reaction was performed with 2-bromopyridine (0.61 mL, 1.0 g, 6.3 mmol), 3-trifluoromethylphenylboronic acid (1.80 g, 9.5 mmol, Alfa Aesar), K_2CO_3 (3.2 g, 23 mmol), and $Pd(PPh_3)_4$ (125 mg, 0.11 mmol). Chromatography was run on silica (20 g) with hexane/CH_2Cl_2 (1/1) to remove impurities, and with hexane/CH_2Cl_2 (1/2) to recover the product. Pale yellow oil: 1.39 g (6.2 mmol, 99%; $C_{12}H_8F_3N$; MW 223.19). ^{1}H NMR (400 MHz, DMSO-d_6): δ = 8.71 (ddd, J = 4.8, 2.0, 1.2 Hz, 1H), 8.43 (s, 1H), 8.39 (d, J = 8.0 Hz, 1H), 8.14–8.08 (m, 1H), 7.94 (td, J = 7.6, 2.0 Hz, 1H), 7.81 (d, J = 8.0 Hz, 1H), 7.74 (t, J = 7.6 Hz, 1H), 7.43 (ddd, J = 7.6, 4.8, 0.8 Hz, 1H) ppm. ^{13}C NMR (100 MHz, CD_2Cl_2): δ = 155.63, 150.06, 140.39, 137.12, 131.10 (q, $J_{C–F}$ = 32 Hz), 130.25 (q, $J_{C–F}$ = 1.3 Hz), 129.45, 125.60 (q, $J_{C–F}$ = 4.0 Hz), 123.84 (q, $J_{C–F}$ = 4.0 Hz), 124.62 (q, $J_{C–F}$ = 271),

123.07, 120.52 ppm. ^{19}F NMR (376 MHz, DMSO-d_6): δ = −61.13 ppm. GC-EI$^+$ MS: *m/z* 223 (M^+, 100%).

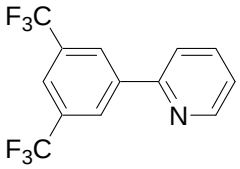

2-(3′,5′-Bis(trifluoromethyl)phenyl)pyridine, L5. The reaction was performed with 2-bromopyridine (0.61 mL, 1.0 g, 6.3 mmol), 3,5-bis(trifluoromethyl)phenylboronic acid (2.45 g, 9.5 mmol, Alfa Aesar), K_2CO_3 (3.1 g, 22 mmol), and $Pd(PPh_3)_4$ (100 mg, 0.087 mmol). Chromatography was run on silica (20 g) with hexane/CH_2Cl_2 (2/1) to remove impurities, and with hexane/CH_2Cl_2 (1/1 to 1/1.5) to recover the product. Pale yellow solid: 1.64 g (5.61 mmol, 89%; $C_{13}H_7F_6N$; MW 291.19). ^{1}H NMR (400 MHz, DMSO-d_6): δ = 8.80–8.74 (m, 3H), 8.36–8.30 (m, 1H), 8.21 (s, 1H), 8.01 (td, *J* = 7.6, 2.0 Hz, 1H), 7.52 (ddd, *J* = 7.6, 4.8, 0.8 Hz, 1H) ppm. ^{19}F NMR (376 MHz, DMSO-d_6): δ = −61.27 ppm.

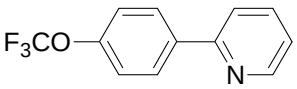

2-(4′-Trifluoromethoxyphenyl)pyridine, L6. The reaction was performed with 2-bromopyridine (0.61 mL, 1.0 g, 6.3 mmol), 4-(trifluoromethoxy)phenylboronic acid (1.96 g, 9.5 mmol, Maybridge), K_2CO_3 (2.6 g, 19 mmol), and $Pd(PPh_3)_4$ (146 mg, 0.13 mmol). Chromatography was done twice (silica, 2×20 g) with hexane/CH_2Cl_2 (1/1) to remove impurities, and with hexane/CH_2Cl_2 (1/2 to 1/3) to recover the product. White solid: 1.12 g (4.68 mmol, 74%; $C_{12}H_8F_3NO$; MW 239.19). ^{1}H NMR (400 MHz, DMSO-d_6): δ = 8.70–8.66 (m, 1H), 8.24–8.18 (m, 2H), 8.03–7.97 (m, 1H), 7.95–7.87 (m, 1H), 7.52–7.44 (m, 2H), 7.42–7.36 (m, 1H) ppm. ^{13}C NMR (100 MHz, Acetone-d_6): δ = 155.47, 149.95, 149.84 (q, $J_{C–F}$ = 1.7 Hz), 138.58, 137.23, 128.66, 122.90, 121.22, 120.81 (q, $J_{C–F}$ = 254 Hz), 120.36 ppm. ^{19}F NMR (188 MHz, DMSO-d_6): δ = −56.7 ppm. GC-EI$^+$ MS: *m/z* 239 (M^+, 100%), 170 ($\{M - CF_3\}^+$, 100%), 154 ($\{M - OCF_3\}^+$, 85%).

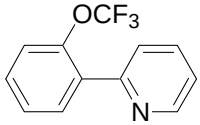

2-(2′-Trifluoromethoxyphenyl)pyridine, L7. The reaction was performed with 2-bromopyridine (0.43 mL, 0.71 g, 4.5 mmol), 2-(trifluoromethoxy)benzeneboronic acid (1.02 g, 5.0 mmol, Aldrich), K_2CO_3 (1.4 g, 10 mmol), and $Pd(PPh_3)_4$ (57 mg, 0.049 mmol). Chromatography was run on silica (20 g) with hexane/CH_2Cl_2 (1/1) to remove impurities, and with hexane/CH_2Cl_2 (1/2 to 1/4) to recover the product. Orange oil: 1.05 g (4.4 mmol, 98%; $C_{12}H_8F_3NO$; MW 239.19). ^{1}H NMR (400 MHz, DMSO-d_6): δ = 8.71 (ddd, *J* = 4.8, 1.6, 0.8 Hz, 1H), 7.91 (td, *J* = 8.0, 2.0 Hz, 1H), 7.79 (dd, *J* = 7.6, 2.0 Hz, 1H), 7.69–7.65 (m, 1H), 7.61–7.47 (m, 3H), 7.42 (ddd, *J* = 7.6, 5.2, 1.2 Hz, 1H) ppm. ^{13}C NMR (100 MHz, DMSO-d_6): δ = 154.49, 150.35, 146.24 (q, $J_{C–F}$ = 1.3 Hz), 137.20, 134.34, 132.40, 131.00, 128.42, 124.84, 123.51, 122.31 (q, $J_{C–F}$ = 1 Hz), 120.67 (q,

$J_{C–F}$ = 255 Hz) ppm. ^{19}F NMR (376 MHz, DMSO-d_6): δ = −56.25 ppm. GC-EI$^+$ MS: *m/z* 239 (M^+, 100%), 170 ({M – CF_3}$^+$, 25%), 154 ({M – OCF_3}$^+$, 75%).

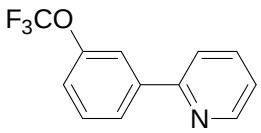

2-(3′-Trifluoromethoxyphenyl)pyridine, L8. The reaction was performed with 2-bromopyridine (0.47 mL, 0.78 g, 4.9 mmol), 3-(trifluoromethoxy)benzeneboronic acid (1.2 g, 5.8 mmol, Alfa Aesar), K_2CO_3 (1.84 g, 13.3 mmol), and $Pd(PPh_3)_4$ (59 mg, 0.051 mmol). Chromatography was run on silica (20 g) with hexane/CH_2Cl_2 (2/1) to remove impurities, and with hexane/CH_2Cl_2 (1/1 to 1/1.5) to recover the product. Colourless oil: 1.17 g (4.9 mmol, 100%; $C_{12}H_8F_3NO$; MW 239.19). ^{1}H NMR (400 MHz, DMSO-d_6): δ = 8.74–8.68 (m, 1H), 8.17–8.11 (m, 1H), 8.11–8.04 (m, 2H), 7.94 (td, *J* = 8.0, 1.6 Hz, 1H), 7.65 (t, *J* = 8.0 Hz, 1H), 7.49–7.40 (m, 2H) ppm. ^{13}C NMR (100 MHz, DMSO-d_6): δ = 154.79, 150.32, 149.71 (q, $J_{C–F}$ = 2.0 Hz), 141.68, 138.06, 131.35, 125.99, 123.98, 121.99, 121.21, 120.83 (q, $J_{C–F}$ = 255 Hz), 119.38 ppm. ^{19}F NMR (376 MHz, DMSO-d_6): δ = −56.64 ppm. GC-EI$^+$ MS: *m/z* 239 (M^+, 100%), 170 ({M – CF_3}$^+$, 25%), 154 ({M – OCF_3}$^+$, 100%).

2. Synthesis of $[(C\hat{}N)_2Ir(\mu\text{-}Cl)]_2$

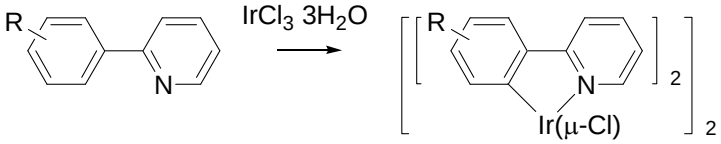

The reactions were performed under argon and in the absence of light. The solvents were de-oxygenated by bubbling with Ar, but they were not dried. $IrCl_3 \cdot 3H_2O$ (150 mg, 0.43 mmol, W. C. Heraeus GmbH) was dissolved in 2-ethoxyethanol/water (3/1 ratio; 6/2 mL) at 60 °C to give purple solution. An excess of the ligand was added. The reaction mixture was stirred at 120°C overnight. It was cooled to RT. If necessary, water was slowly added to the stirred reaction mixture to precipitate the product. The product was filtered and washed with ethanol/water (1/1), water, ethanol/water (1/1) again, and hexane. Further details are provided below.

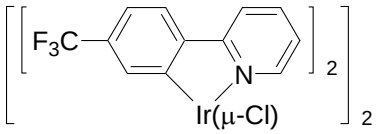

$[(L1)_2Ir(\mu\text{-}Cl)]_2$. $IrCl_3 \cdot 3H_2O$ (150 mg, 0.43 mmol) and **L1** (214 mg, 0.96 mmol) gave orange-yellow solution. The product was precipitated with water (3 mL). Bright yellow solid: 106 mg (0.079 mmol, 37%; $C_{48}H_{28}Cl_2F_{12}Ir_2N_4$; MW 1344.08). ^{1}H NMR (400 MHz, CD_2Cl_2): δ = 9.23 (dd, J = 6.0, 0.8 Hz, 4H), 8.09 (d, J = 7.6 Hz, 4H), 7.97 (dt, J = 8.0, 1.6 Hz, 4H), 7.71 (d, J = 8.4 Hz, 4H), 7.12 (dd, J = 8.0, 1.2 Hz, 4H), 7.04–6.98 (m, 4H), 6.12 (s, 4H) ppm. ^{19}F NMR (376 MHz, CD_2Cl_2): δ = −63.26 ppm. For the scaled-up procedure, $IrCl_3 \cdot 3H_2O$ (300 mg, 0.85 mmol) and **L1** (418 mg, 1.87 mmol) in 2-ethoxyethanol/water (6/2 mL) gave, after precipitation with water (4 mL), 367 mg (0.273 mmol, 64%) of the product.

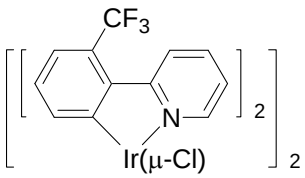

$[(L2)_2Ir(\mu\text{-}Cl)]_2$. $IrCl_3 \cdot 3H_2O$ (150 mg, 0.43 mmol) and **L2** (214 mg, 0.96 mmol) gave orange suspension. The product was precipitated with water (1 mL). Yellow solid: 180 mg (0.134 mmol, 62%; $C_{48}H_{28}Cl_2F_{12}Ir_2N_4$; MW 1344.08). The compound is insoluble in CH_2Cl_2 or acetone.

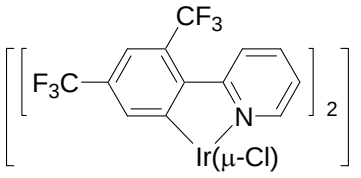

$[(L3)_2Ir(\mu\text{-}Cl)]_2$. $IrCl_3 \cdot 3H_2O$ (150 mg, 0.43 mmol) and **L3** (279 mg, 0.96 mmol) gave yellow-orange suspension. The product was precipitated with water (2 mL). Yellow-orange solid: 247 mg (0.153 mmol, 71%; $C_{52}H_{24}Cl_2F_{24}Ir_2N_4$; MW 1616.07). ^{1}H NMR (400 MHz, CD_2Cl_2): δ = 9.20 (dd, J = 5.6, 1.2 Hz, 4H), 8.49 (d, J = 8.4 Hz, 4H), 8.10–8.00 (m, 4H), 7.52 (s, 4H), 7.12–

7.03 (m, 4H), 6.08 (s, 4H) ppm. ^{19}F NMR (376 MHz, CD_2Cl_2): δ = −57.65 (12F), −63.86 (12F) ppm.

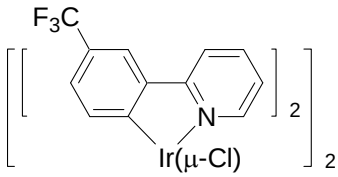

[(L4)$_2$Ir(μ-Cl)]$_2$. $IrCl_3 \cdot 3H_2O$ (150 mg, 0.43 mmol) and **L4** (214 mg, 0.96 mmol) gave yellow suspension. Yellow solid: 187 mg (0.14 mmol, 65%; $C_{48}H_{28}Cl_2F_{12}Ir_2N_4$; MW 1344.08). ^{1}H NMR (400 MHz, CD_2Cl_2): δ = 9.23 (ddd, J = 6.0, 1.6, 0.8 Hz, 4H), 8.08 (dd, J = 8.0, 0.8 Hz, 4H), 7.95 (td, J = 7.6, 1.6 Hz, 4H), 7.82 (s, 4H), 7.01–6.94 (m, 4H), 6.89–6.83 (m, 4H), 6.03 (d, J = 8.4 Hz, 4H) ppm. ^{19}F NMR (376 MHz, CD_2Cl_2): δ = −62.47 ppm. For the scaled-up procedure, $IrCl_3 \cdot 3H_2O$ (300 mg, 0.85 mmol) and **L4** (428 mg, 1.92 mmol) in 2-ethoxyethanol/water (6/2 mL) gave 418 mg (0.31 mmol, 73%) of the product.

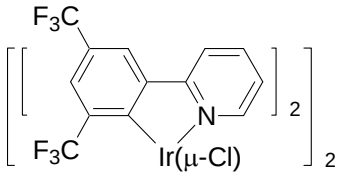

[(L5)$_2$Ir(μ-Cl)]$_2$. $IrCl_3 \cdot 3H_2O$ (150 mg, 0.43 mmol) and **L5** (279 mg, 0.96 mmol) gave yellow solution. Water (5 mL) was added. The product separated as an oil that solidified on sonication and stirring. Pale yellow solid: 286 mg (0.177 mmol, 82%; $C_{52}H_{24}Cl_2F_{24}Ir_2N_4$; MW 1616.07). ^{1}H NMR (400 MHz, CD_2Cl_2): δ = 8.47 (d, J = 6.0 Hz, 1H), 8.02 (s, 1H), 7.96 (d, J = 8.0 Hz, 1H), 7.89 (td, J = 7.6, 1.6 Hz, 1H), 7.34 (s, 1H), 6.67–6.60 (m, 1H) ppm. ^{19}F NMR (376 MHz, CD_2Cl_2): δ = −58.21 (12F), −62.84 (12F) ppm.

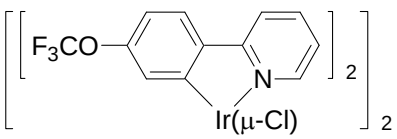

[(L6)$_2$Ir(μ-Cl)]$_2$. $IrCl_3 \cdot 3H_2O$ (150 mg, 0.43 mmol) and **L6** (229 mg, 0.96 mmol) gave yellow solution. The product was precipitated with water (2 mL). Yellow solid: 207 mg (0.147 mmol, 68%; $C_{48}H_{28}Cl_2F_{12}Ir_2N_4O_4$; MW 1408.08). ^{1}H NMR (400 MHz, CD_2Cl_2): δ = 9.18 (d, J = 4.8 Hz, 4H), 7.97 (d, J = 7.6 Hz, 4H), 7.89 (td, J = 8.0, 1.6 Hz, 4H), 7.63 (d, J = 8.4 Hz, 4H), 6.95–6.88 (m, 4H), 6.77–6.71 (m, 4H), 5.67 (d, J = 1.2 Hz, 4H) ppm. ^{19}F NMR (376 MHz, CD_2Cl_2): δ = −57.7 ppm.

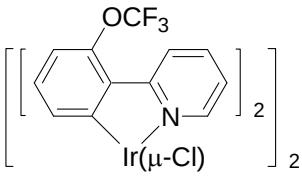

[(L7)$_2$Ir(μ-Cl)]$_2$. $IrCl_3 \cdot 3H_2O$ (150 mg, 0.43 mmol) and **L7** (229 mg, 0.96 mmol) gave greenish-yellow suspension. Greenish-yellow solid: 227 mg (0.161 mmol, 75%; $C_{48}H_{28}Cl_2F_{12}Ir_2N_4O_4$; MW 1408.08). The compound is insoluble in CH_2Cl_2 or acetone.

Attempted synthesis of $[(L8)_2Ir(\mu\text{-}Cl)]_2$. The reaction was performed as described above for **L1**–**L7**. $IrCl_3 \cdot 3H_2O$ (150 mg, 0.43 mmol) and **L8** (229 mg, 0.96 mmol) gave yellow suspension. Yellow solid: 80 mg (0.057 mmol, 26%; $C_{48}H_{28}Cl_2F_{12}Ir_2N_4O_4$; MW 1408.08). ^{1}H NMR (400 MHz, CD_2Cl_2 or DMSO-d_6) and ^{19}F NMR indicate that the solid is a mixture of complexes. ^{19}F NMR (376 MHz, CD_2Cl_2): δ = −56.85, −58.46 (major), −58.46, −58.47, −58.51 ppm. ^{19}F NMR (376 MHz, DMSO-d_6): δ = −54.89, −56.76 (major), −56.79, −56.87 (major) ppm {in DMSO, the dimer is expected to react with the solvent to form the monomer $[(C\text{^}N)_2Ir(Cl)(DMSO)]$}.

3. X-Ray Crystallography

Single crystals for X-ray analysis were grown by slow evaporation of a mixed solution of CH_2Cl_2/hexane for **1**, **4**, and **7**; by vapour diffusion of ether into the concentrated CH_2Cl_2 solution for **5**; and by vapour diffusion of ether into the concentrated acetone solution for **6**.

The diffraction data were measured at 100(2) K using Mo K_α radiation on a Bruker APEX II CCD diffractometer equipped with a kappa geometry goniometer. All datasets were reduced by EvalCCD[1] and then corrected for absorption.[2] The solutions and refinements were performed by SHELX.[3] The crystal structures were refined using full-matrix least-squares based on F^2 with all non H-atoms anisotropically defined. Hydrogen atoms were placed in calculated positions by means of the "riding" model.

Several rotational disorder problems were found during the last stages of refinement for all crystal structures and they were treated by the split model combined with some restraints (SIMU, DFIX, SADI cards). Small twin components were discovered by TWINROTMAT[4] in the case of **1** and **6**, whereas SQUEEZE[4] was applied in the case of **5**.

Table S1. Crystal Data and Structure Refinement for Ir(III) Complexes.

compound	**1**	**4**	**5**	**6**	**7**
empirical formula	$C_{35}H_{32}F_9IrN_4O_3S\cdot CH_2Cl_2$	$C_{35}H_{32}F_9IrN_4O_3S$	$C_{37}H_{30}F_{15}IrN_4O_3S$	$C_{35}H_{32}F_9IrN_4O_5S$	$C_{35}H_{32}F_9IrN_4O_5S$
fw	1036.83	951.91	1087.91	983.91	983.91
temp [K]	100(2)	100(2)	100(2)	100(2)	100(2)
wavelength [Å]	0.71073	0.71073	0.71073	0.71073	0.71073
cryst syst	monoclinic	orthorhombic	triclinic	triclinic	orthorhombic
space group	$P2_1/n$	*Pbca*	*P*-1	*P*-1	*Pbca*
unit cell dimensions	a = 13.221(2) Å b = 13.629(2) Å c = 22.862(5) Å α = 90° β = 95.200(13)° γ = 90°	a = 11.3575(16) Å b = 18.976(2) Å c = 35.022(3) Å α = 90° β = 90° γ = 90°	a = 14.4301(18) Å b = 16.0365(16) Å c = 20.574(4) Å α = 97.072(11)° β = 106.481(10)° γ = 104.780(9)°	a = 13.4577(18) Å b = 13.602(2) Å c = 22.574(4) Å α = 102.632(15)° β = 95.986(11)° γ = 91.729(13)°	a = 13.3214(12) Å b = 19.264(5) Å c = 30.362(6) Å α = 90° β = 90° γ = 90°
vol [Å]^3	4102.8(13)	7547.9(15)	4315.1(11)	4004.2(11)	7792(3)
Z	4	8	4	4	8
ρ (calc) [Mg/m^3]	1.679	1.675	1.675	1.632	1.677
μ [mm^{-1}]	3.516	3.677	3.247	3.472	3.569
F(000)	2040	3744	2128	1936	3872
cryst size [mm^3]	0.40 × 0.20 × 0.13	0.48 × 0.28 × 0.21	0.50 × 0.41 × 0.40	0.44 × 0.18 × 0.17	0.47 × 0.17 × 0.16
θ range	3.07 – 27.53°	3.49 – 25.00°	3.04 – 27.50°	3.01–30.03°	3.06 – 27.50°
index ranges	$-17 \le h \le 17$ $-17 \le k \le 17$ $-5 \le l \le 29$	$-13 \le h \le 12$ $-22 \le k \le 22$ $-41 \le l \le 41$	$-16 \le h \le 18$ $-20 \le k \le 20$ $-26 \le l \le 26$	$-18 \le h \le 18$ $-19 \le k \le 19$ $-31 \le l \le 31$	$-17 \le h \le 16$ $-24 \le k \le 24$ $-39 \le l \le 39$
reflns collected	9315	90603	73313	22948	112442
independent reflns	9315 [R(int) = 0.0000]	6617 [R(int) = 0.0271]	19244 [R(int) = 0.0215]	22948 [R(int) = 0.0000]	8930 [R(int) = 0.0679]
completeness to θ	27.53° – 98.5%	25.00° – 99.4%	25.00° – 98.4%	30.03° – 98.0%	27.50° – 99.8%
absorption correction	semi-empirical from equivalents	semi-empirical from equivalents	semi-empirical from equivalents	semi-empirical from equivalents	semi-empirical from equivalents
max/min transm	0.7456 / 0.3873	0.7452 / 0.4471	0.7456 / 0.6424	0.7460 / 0.4801	0.7456 / 0.4366
refinement method	full-matrix least-squares on F^2	full-matrix least-squares on F^2	full-matrix least-squares on F^2	full-matrix least-squares on F^2	full-matrix least-squares on F^2
data/restraints/params	9315 / 84 / 537	6617 / 24 / 536	19244 / 414 / 1321	22948 / 817 / 1344	8930 / 144 / 559
GOF on F^2	1.327	1.224	1.150	1.239	1.336
final R indices [$I > 2\sigma(I)$]	R1 = 0.0927, wR2 = 0.2594	R1 = 0.0159, wR2 = 0.0367	R1 = 0.0303, wR2 = 0.0695	R1 = 0.0617, wR2 = 0.1496	R1 = 0.0443, wR2 = 0.0880
R indices (all data)	R1 = 0.1056, wR2 = 0.2672	R1 = 0.0182, wR2 = 0.0381	R1 = 0.0501, wR2 = 0.0817	R1 = 0.0771, wR2 = 0.1605	R1 = 0.0670, wR2 = 0.0979
largest diff. peak/hole [e/Å^3]	6.838 / −5.079	0.418 / −0.476	2.596 / −1.322	7.137 / −4.285	3.058 / −2.047

4. Electrochemistry

Electrochemical experiments were conducted in DMF (99.8%, Extra Dry, over Molecular Sieves, AcroSeal®, Acros) or acetonitrile (99.9%, Extra Dry, over Molecular Sieves, AcroSeal®, Acros), with 0.1 M tetra-*n*-butylammonium hexafluorophosphate (Fluka, electrochemical grade) as the supporting electrolyte, with a PC controlled AutoLab PSTAT10 electrochemical workstation.

The experiments were carried out under argon in an electrochemical cell through which a stream of Ar was passed (the flow of Ar was stopped during the measurement to prevent stirring of the solution). Glassy carbon, platinum spiral, and platinum wire served as working, counter, and quasi-reference electrodes. Ferrocene was added as an internal reference at the end of each experiment. Estimated error: ±50 mV. The anodic/cathodic peak separation for the standard (Fc^+/Fc couple) at 100 mV/s was 73–93 mV. Cyclic voltammetry was performed at scan rates of 1 and 0.1 V/s.

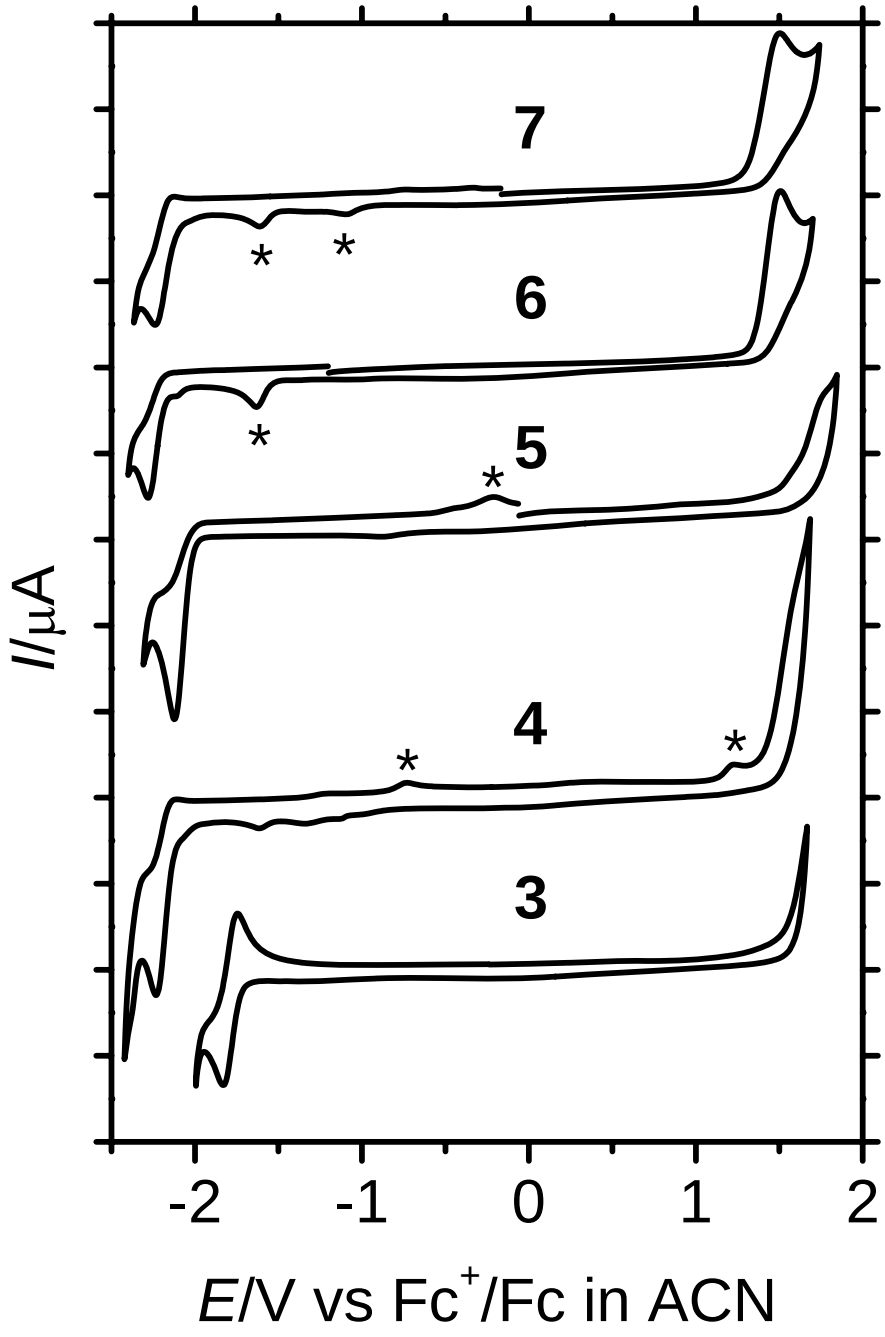

Figure S1. Cyclic voltammograms of **3**–**7** in acetonitrile (glassy carbon working electrode, 0.1 M NBu_4PF_6, 100 mV/s). The symbol (*) marks return waves of irreversible processes. The unit on the vertical axis is 20 μA.

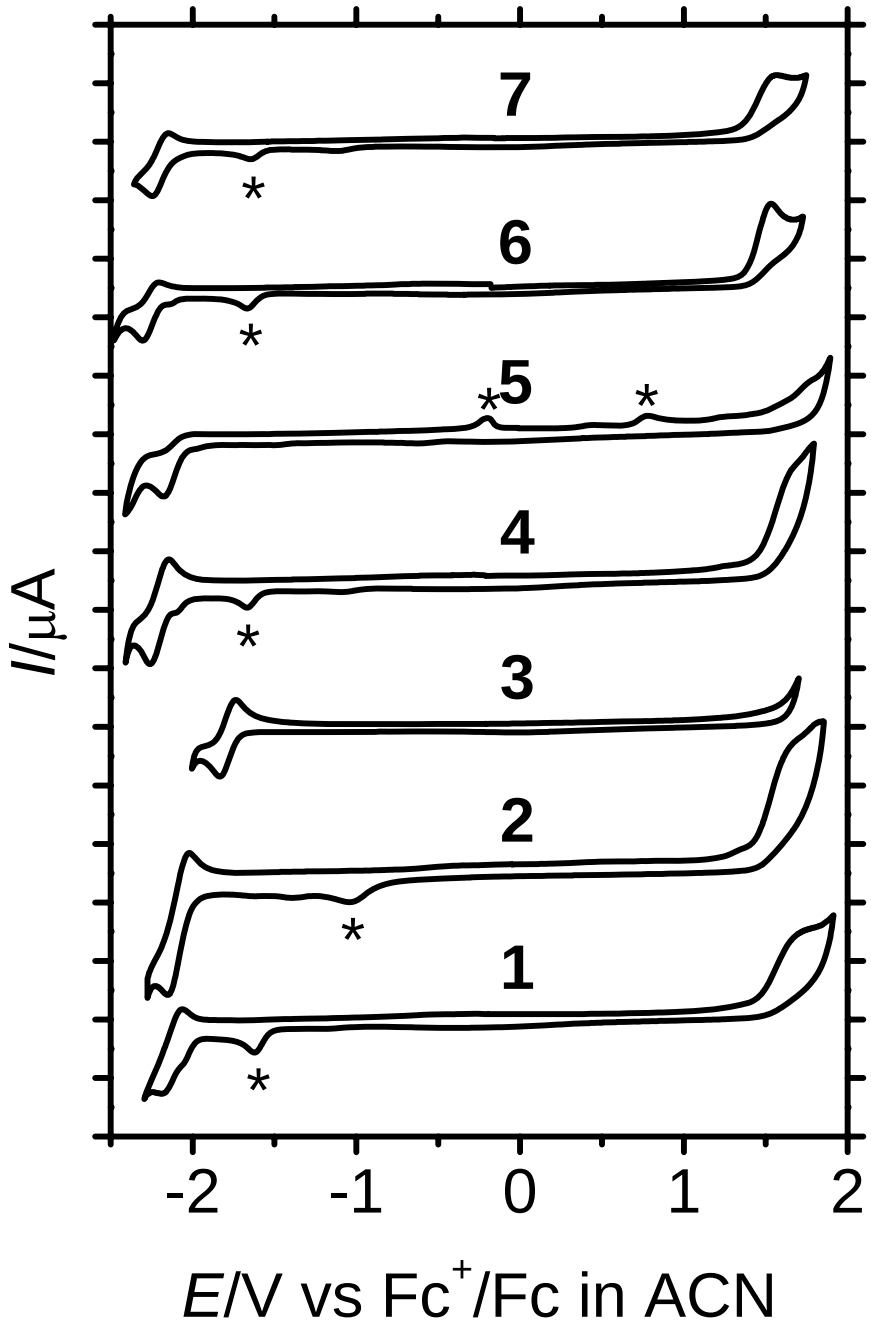

Figure S2. Cyclic voltammograms of **1**–**7** in acetonitrile (glassy carbon working electrode, 0.1 M NBu_4PF_6, 1 V/s). The symbol (*) marks return waves of irreversible processes. The unit on the vertical axis is 100 μA.

Table S2. Redox Properties of **1**–**7** in Acetonitrile at Scan Rate of 1 V/s[a]

complex	R′[b]	E^{red}, V[c]	E^{ox}, V[c]	ΔE, V[d]
1	4′-CF_3	−2.12 (122)		
2	2′-CF_3	−2.08 (127)		
3	2′,4′-$(CF_3)_2$	−1.78 (98)		
4	3′-CF_3	−2.20 (112)		
5	3′,5′-$(CF_3)_2$	−2.17		
6	4′-OCF_3	−2.26 (98)	1.53	3.79
7	2′-OCF_3	−2.19 (98)	1.56	3.76

[a]Relative to Fc^+/Fc. On glassy carbon working electrode, in the presence of 0.1 M $(NBu_4)PF_6$, at scan rate 1 V/s. Estimated error: ±50 mV. The anodic/cathodic peak separation for the standard, Fc^+/Fc couple, was 78–93 mV.

[b]Substituents on the phenyl ring of the cyclometalating ligand.

[c]Irreversible process (unless stated otherwise); the oxidation or reduction peak potentials are reported. Reduction at 1 V/s is a reversible or quasi-reversible process (except for **5**); $E_{1/2}{}^{red}$ is reported; the anodic/cathodic peak separation is given in brackets. Oxidation of the complexes was outside of the electrochemical window for **1**–**5** in acetonitrile (> 1.5 V relative to Fc^+/Fc).

[d]Redox gap: $\Delta E = E^{ox} - E^{red}$.

5. Spectroscopy

Infrared absorption spectra of solid films of the complexes were recorded with a Digilab FTS 7000 FT-IR Spectrometer in reflectance mode with background subtraction at atmospheric pressure and at room temperature. The films were formed by evaporation of dichloromethane solution of the complex on a diamond window. The thickness of the films was not controlled. When necessary, the higher absorbance was achieved by evaporating more of the solution of the complex on top of the existing film.

Electronic absorption spectra were recorded with an HP/Agilent 8453 Diode Array UV/VIS spectrophotometer under air in optical cells of 2 or 10 mm path length. The solutions in CH_2Cl_2 (Sigma-Aldrich, puriss p.a., ACS reagent) were freshly prepared before experiment.

The luminescence measurements were conducted in fluorescence cuvettes of 1 cm path length. The liquid samples were purged from oxygen by bubbling with argon for 15 min. The uncorrected emission spectra were recorded with an Edinburgh Instruments FLS920 spectrometer with a Peltier-cooled Hamamatsu R928 photomultiplier tube (185-850 nm). An Edinburgh Instruments Xe900 450 W xenon arc lamp was a source of excitation light. The corrected emission spectra were calculated by applying a calibration curve supplied with the instrument. Luminescence quantum yields (Φ) in solution were calculated by the method of Demas and Crosby[5] from the corrected spectra on a wavelength scale (nm) using an air-equilibrated solution of quinine sulfate in 1 N H_2SO_4 (Φ = 54.6%).[6]

Emission lifetimes in the nanosecond to microsecond range were measured by a single photon counting technique with the same Edinburgh Instruments FLS920 spectrometer, a laser diode as an excitation source (1 MHz; λ_{exc} = 407 nm; 200 ps time resolution after de-convolution), and the above-mentioned PMT as a detector. Alternatively, the lifetimes were measured with an IBH single photon counting spectrometer equipped either with a thyratron gated nitrogen lamp (2 to 40 kHz; λ_{exc} = 337 nm; 0.5 ns time resolution) or pulsed NanoLED excitation sources (λ_{exc} at 278, 331, 465, and 560 nm; pulse width $\leq$ 0.3 ns); the detector was a red-sensitive (185–850 nm) Hamamatsu R-3237-01 PMT. Analysis of the luminescence decay profiles was accomplished with the DAS6 Decay Analysis Software provided by the manufacturer.

The luminescence lifetimes in the microsecond to millisecond range were measured with a Perkin-Elmer LS-50 spectrofluorimeter with a pulsed xenon lamp with a variable repetition rate, and were calculated with standard software. The luminescence spectra at 77 K were recorded in a glass tube (2 mm in diameter) placed in a quartz Dewar flask filled with liquid nitrogen.

For solid samples, the luminescence quantum yields were calculated by the method of De Mello *et al*.[7] from the corrected emission spectra recorded in a barium sulphate coated integrating sphere (6 inch in diameter), using He-Cd laser as a light source (λ_{exc} = 325 nm; 5 mW), and a CCD AVA-Spec2048 or R928 PMT, as a detector.

The PMMA films containing 1% wt. of the complex were drop-cast from dichloromethane solutions. The neat films of the complexes were spin coated from acetonitrile solutions. The thickness of the films was not controlled.

Experimental errors are estimated to be ±8% for lifetime determinations; ±20% for emission quantum yields; ±2 nm and ±5 nm for absorption and emission maxima.

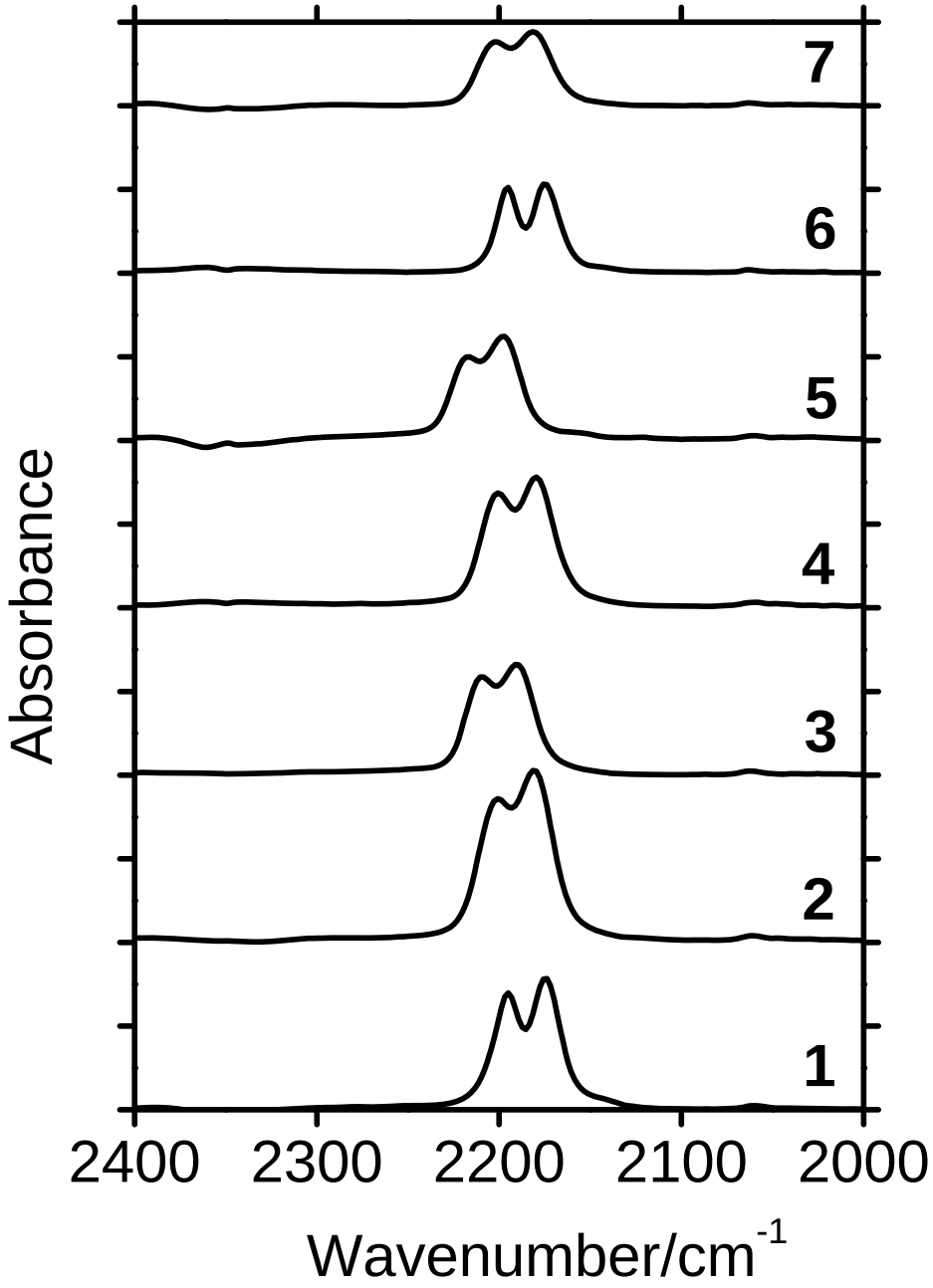

Figure S3. Infrared absorption of solid films of neat complexes **1**–**7** in the range of transitions associated with the stretching vibrations of C≡N bond. The unit on the vertical axis is 0.1.

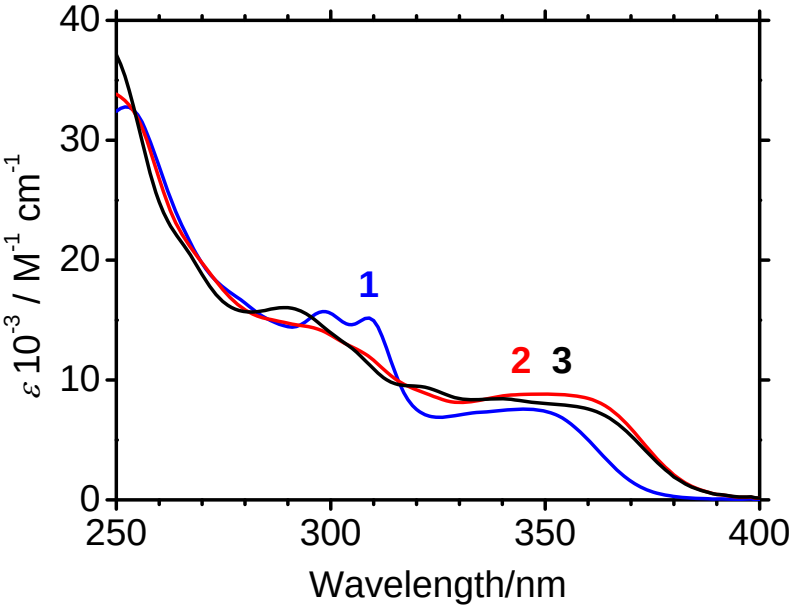

Figure S4. Absorption spectra of **1** (9.37×10^{-5} M), **2** (8.44×10^{-5} M), and **3** (6.36×10^{-5} M) in dichloromethane.

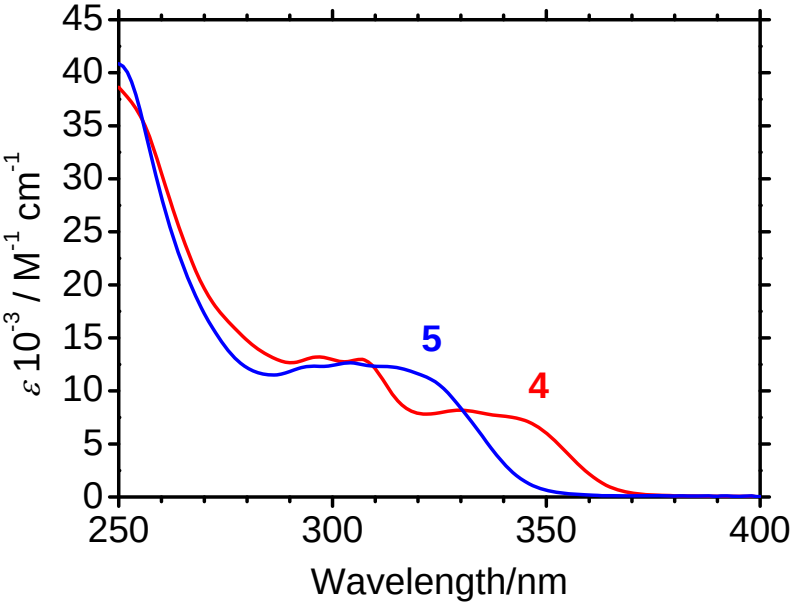

Figure S5. Absorption spectra of **4** (7.82×10^{-5} M) and **5** (7.02×10^{-5} M) in dichloromethane.

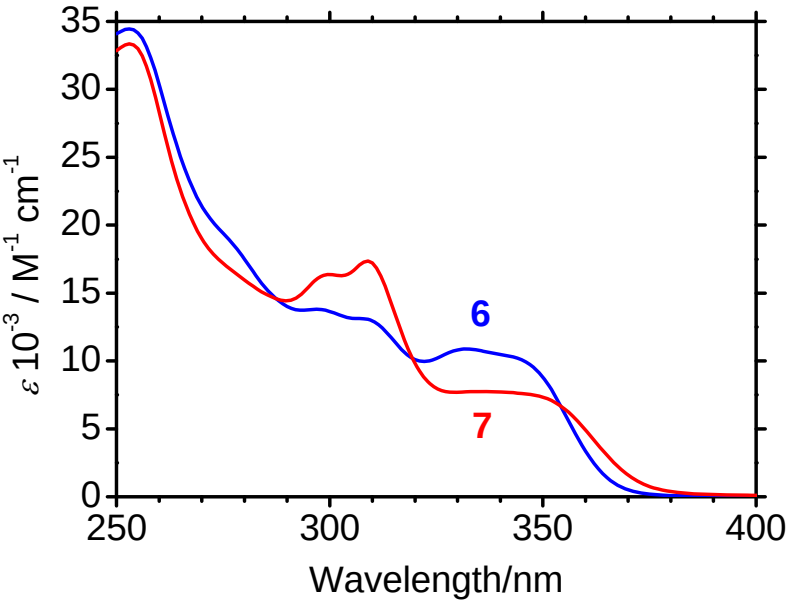

Figure S6. Absorption spectra of **6** (7.03×10^{-5} M) and **7** (6.79×10^{-5} M) in dichloromethane.

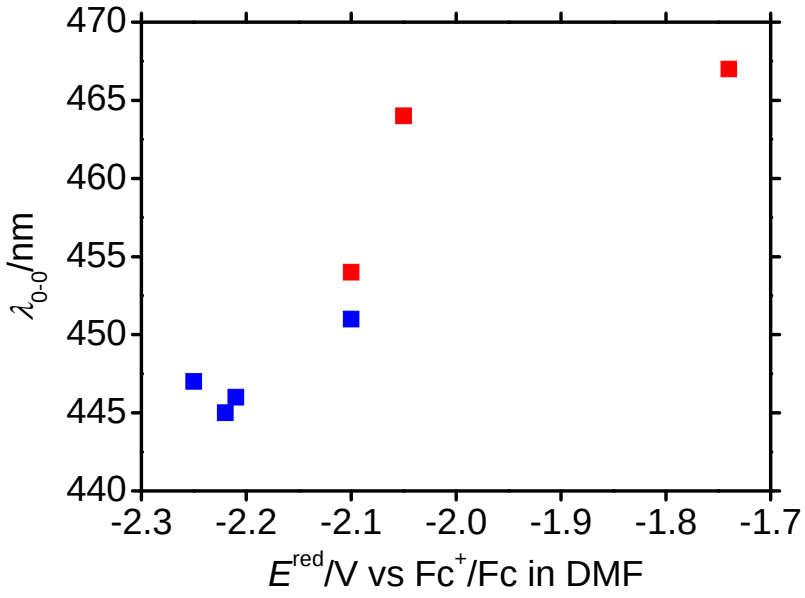

Figure S7. Correlation between the reduction potential (DMF, 100 mV/s, Table 2) and the wavelength of 0–0 transition (λ_{0-0} at 77 K in dichloromethane, Table 4) for complexes **1**–**7**. Red squares refer to $E_{1/2}^{red}$ of reversible/quasi-reversible reduction of **1**–**3**. Blue squares refer to E^{red} of irreversible reduction of **4**–**7**.

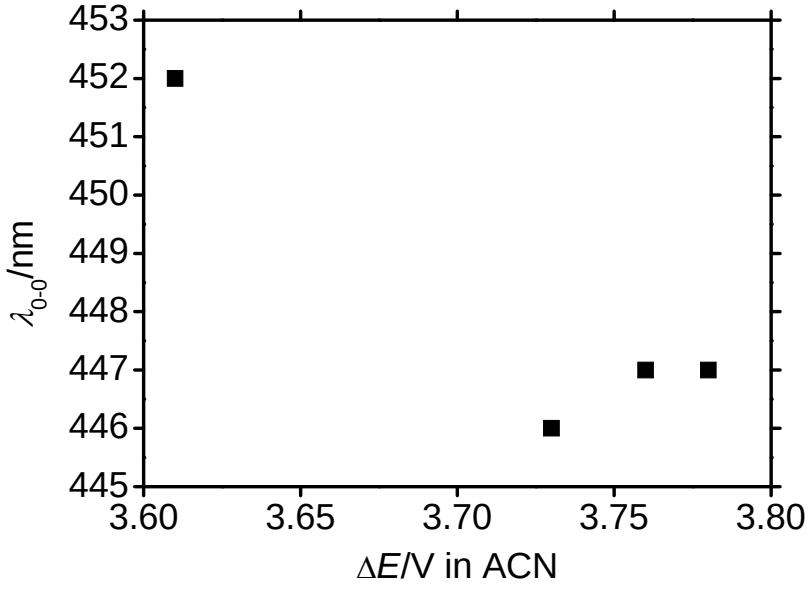

Figure S8. Correlation between the redox gap (acetonitrile, 100 mV/s, Table 2) and the wavelength of 0–0 transition (λ_{0-0} at 77 K in dichloromethane, Table 4) for **6**, **7**, **9H**, and **9F**.

6. References

(1) Duisenberg, A. J. M.; Kroon-Batenburg, L. M. J.; Schreurs, A. M. M. *J. Appl. Cryst.* **2003**, *36*, 220.
(2) Blessing, R. H. *Acta Cryst.* **1995**, *A51*, 33.
(3) Sheldrick**,** G. M. *Acta Cryst.* **2008**, *A64*, 112.
(4) Spek, A. L. *Acta Cryst.* **2009**, *D65*, 148.
(5) Demas, J. N.; Crosby, G. A. *J. Phys. Chem.* **1971**, *75*, 991.
(6) Meech, S. R.; Phillips, D. *J. Photochem.* **1983**, *23*, 193.
(7) De Mello, J. C.; Wittmann, H. F.; Friend, R. H. *Adv. Mater*. **1997**, *9*, 230.

7-A. 2-(4′-Trifluoromethylphenyl)pyridine L1, $[(L1)_2Ir(\mu\text{-}Cl)]_2$, 1

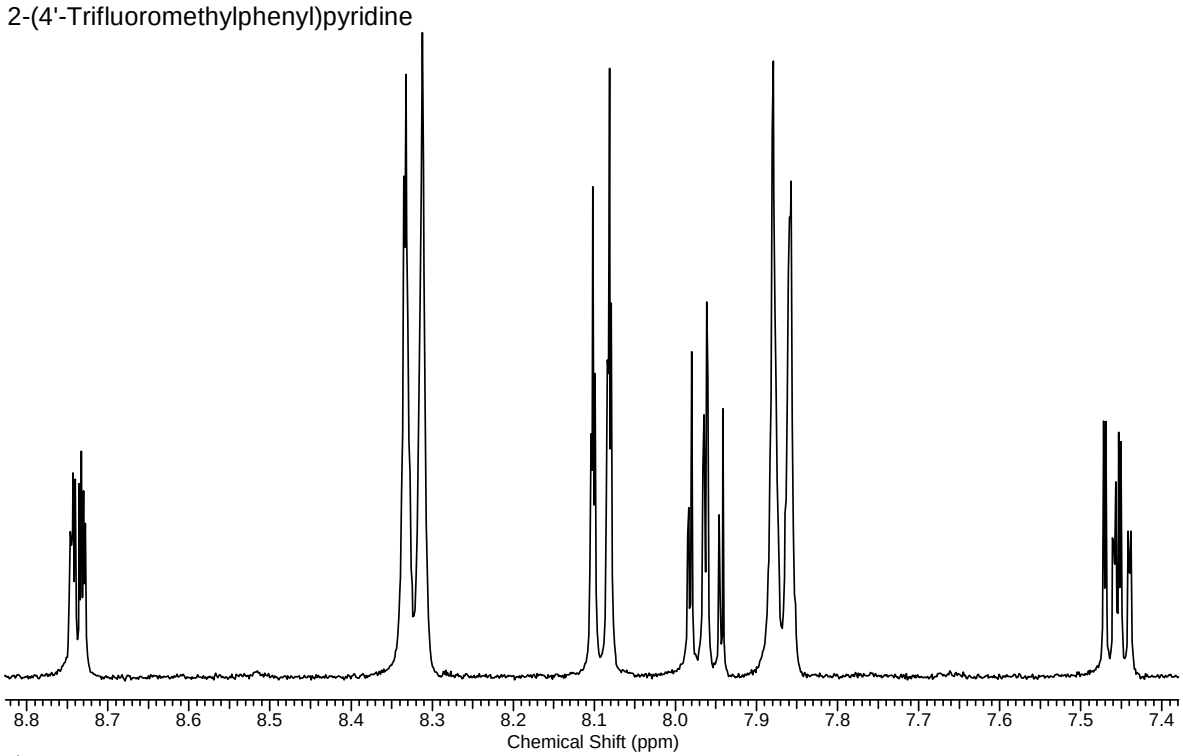

^{1}H NMR Spectrum of 2-(4′-trifluoromethylphenyl)pyridine in DMSO-d_6.

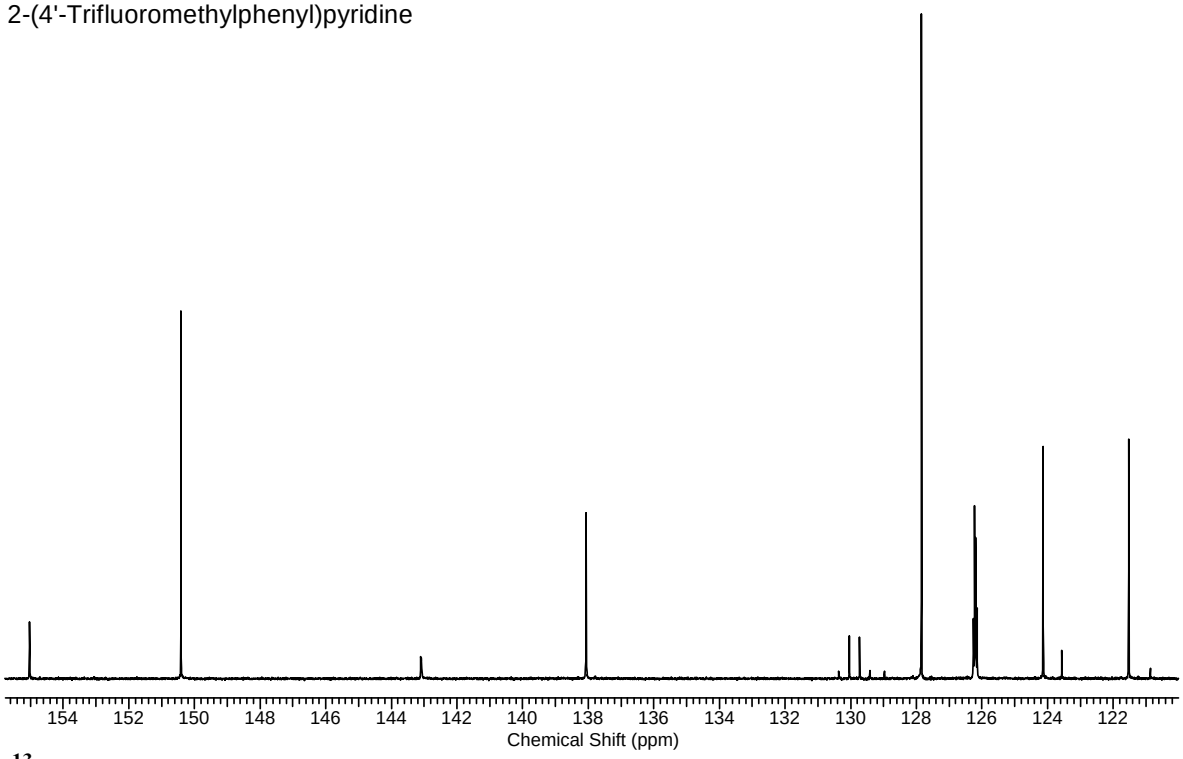

^{13}C NMR Spectrum of 2-(4′-trifluoromethylphenyl)pyridine in DMSO-d_6.

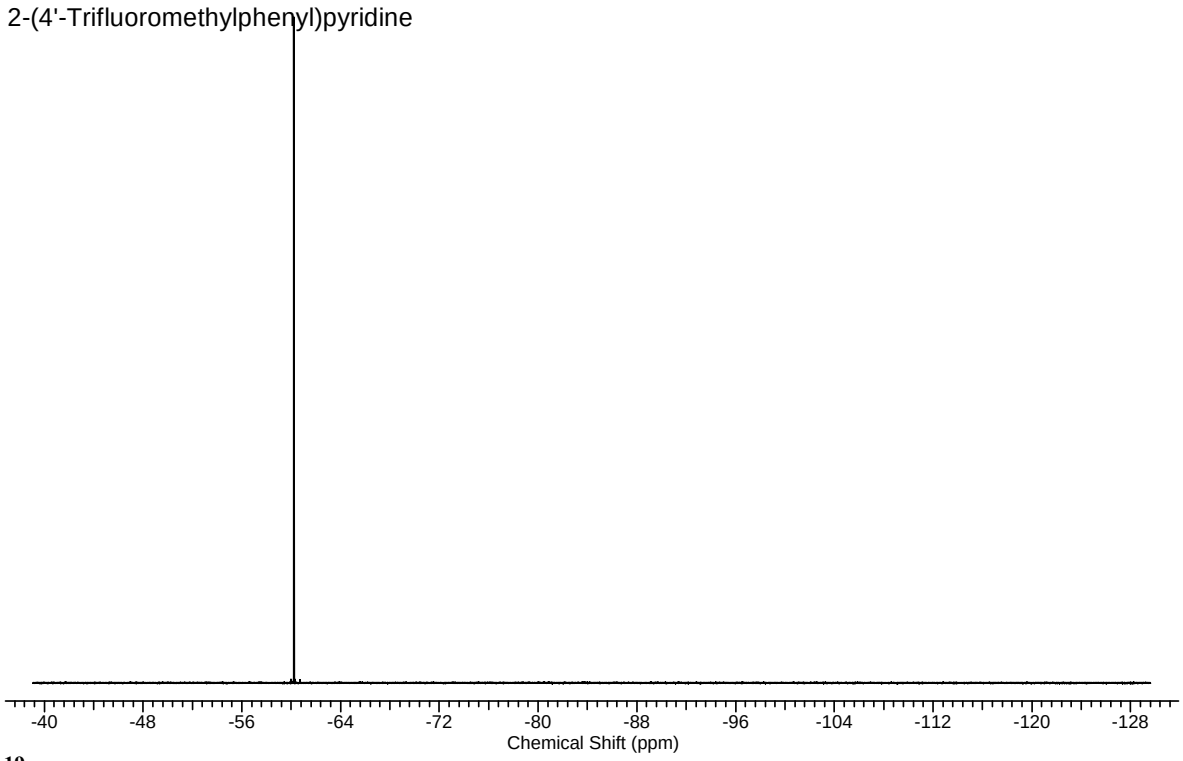

^{19}F NMR Spectrum of 2-(4′-trifluoromethylphenyl)pyridine in DMSO-d_6.

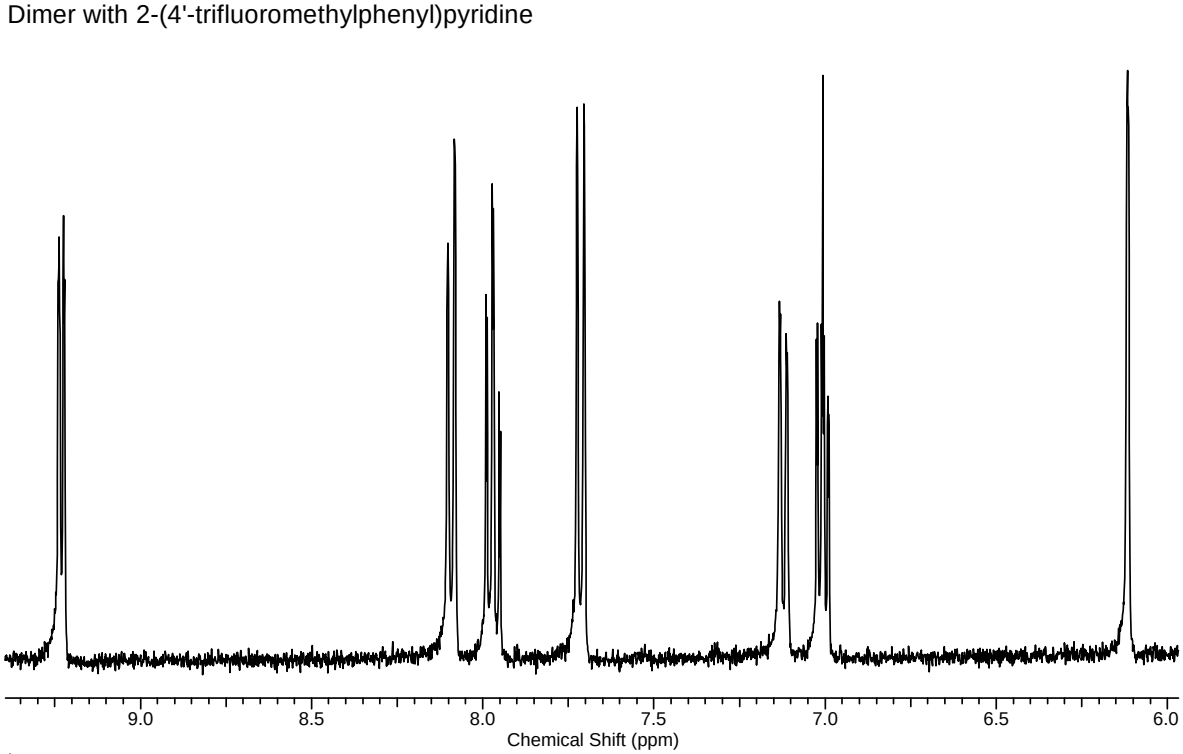

^{1}H NMR Spectrum of $[(C\hat{}N)_2Ir(\mu\text{-}Cl)]_2$ for 2-(4′-trifluoromethylphenyl)pyridine in CD_2Cl_2.

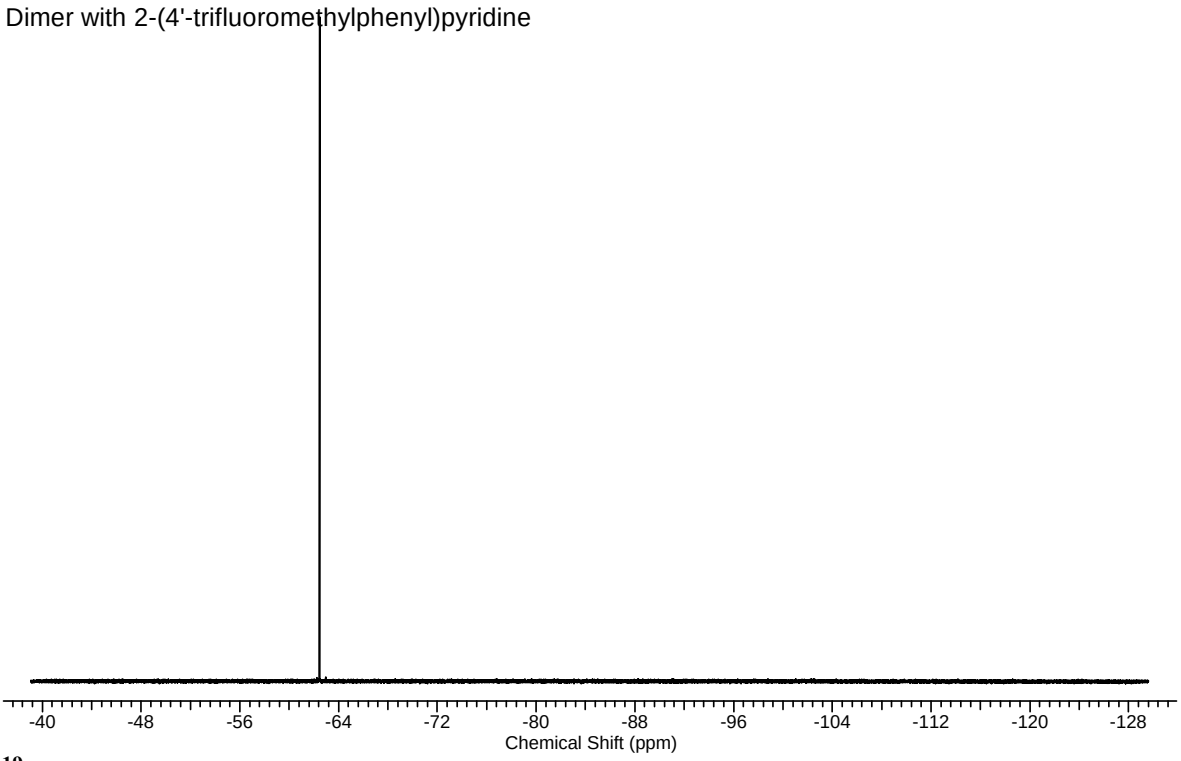

^{19}F NMR Spectrum of $[(C^N)_2Ir(\mu\text{-}Cl)]_2$ for 2-(4′-trifluoromethylphenyl)pyridine in CD_2Cl_2.

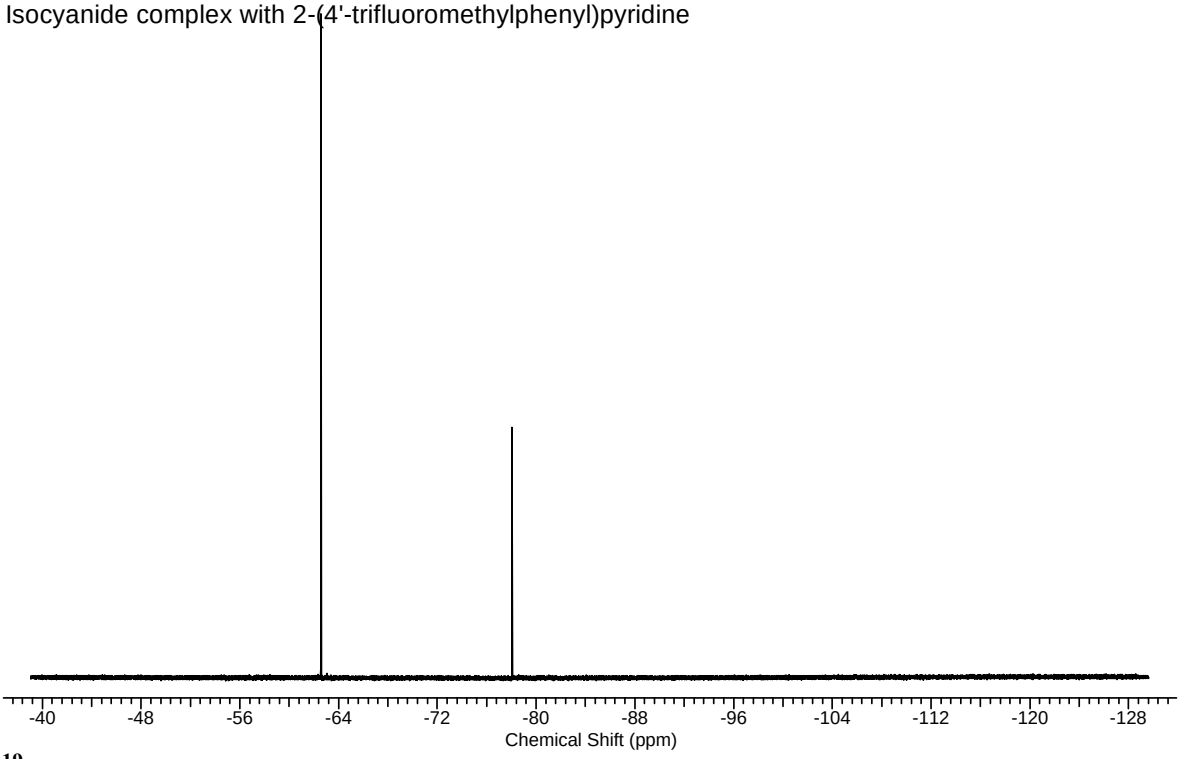

^{19}F NMR Spectrum of isocyanide complex with 2-(4′-trifluoromethylphenyl)pyridine in CD_2Cl_2.

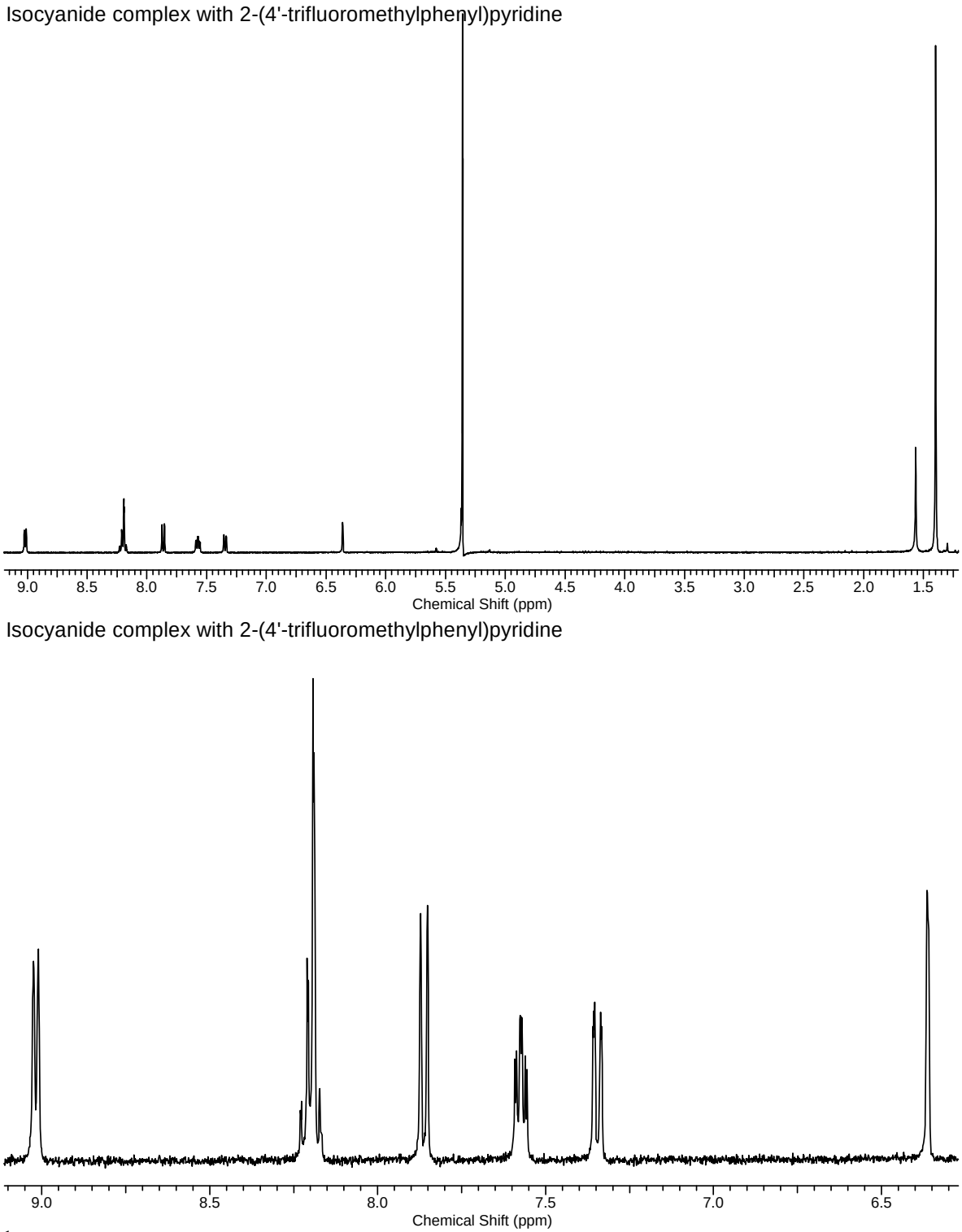

^{1}H NMR Spectrum of isocyanide complex with 2-(4′-trifluoromethylphenyl)pyridine in CD_2Cl_2 (top, complete; bottom, arom. H).

7-B. 2-(2′-Trifluoromethylphenyl)pyridine L2, $[(L2)_2Ir(\mu\text{-}Cl)]_2$, 2

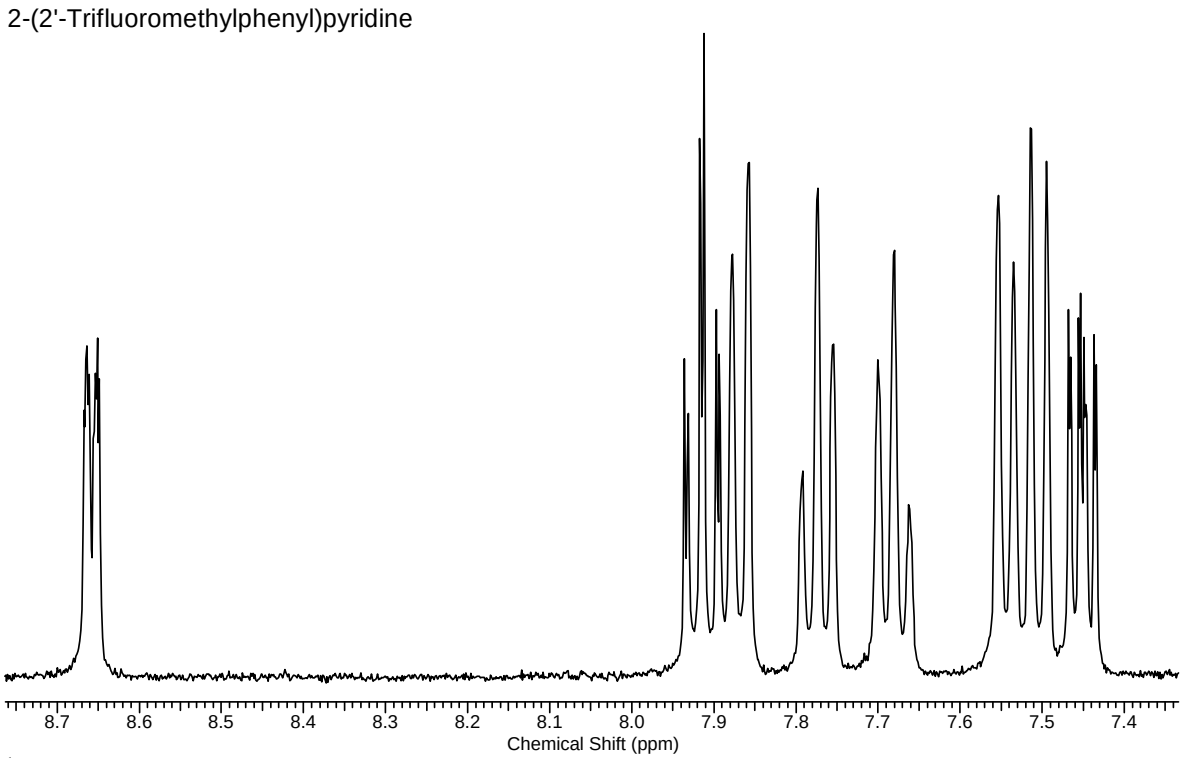

^{1}H NMR Spectrum of 2-(2′-trifluoromethylphenyl)pyridine in DMSO-d_6.

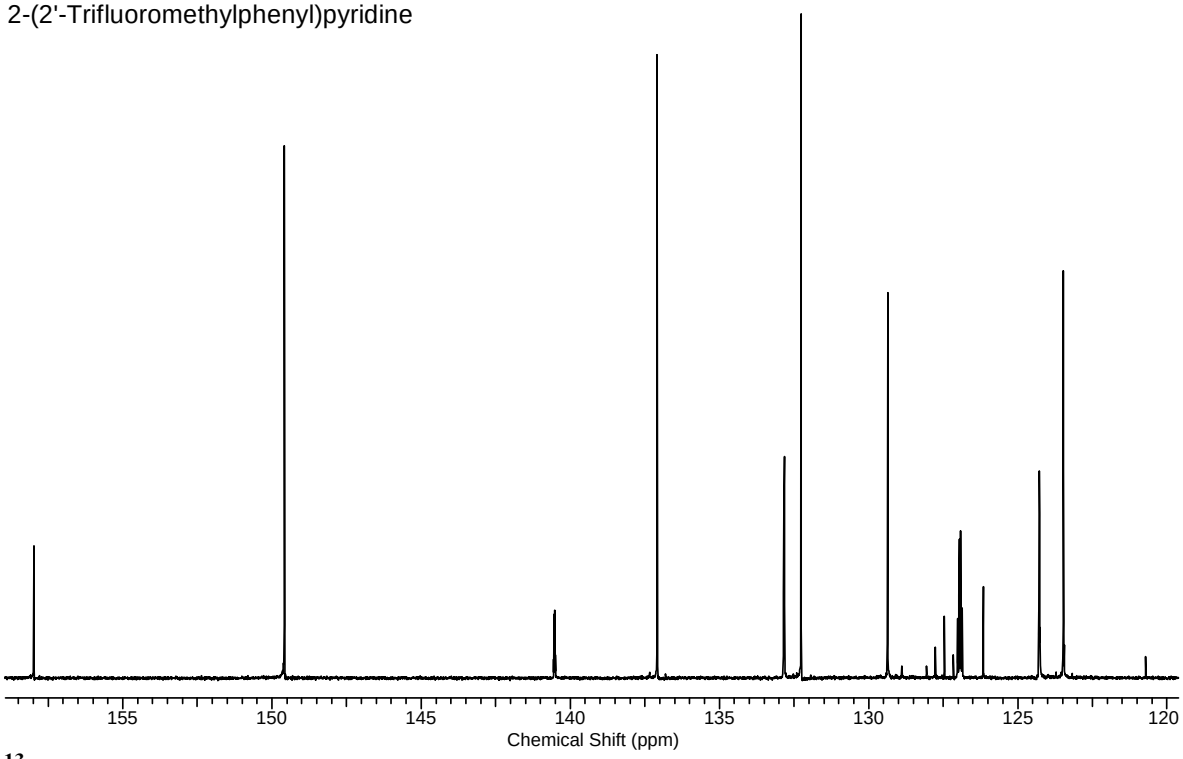

^{13}C NMR Spectrum of 2-(2′-trifluoromethylphenyl)pyridine in DMSO-d_6.

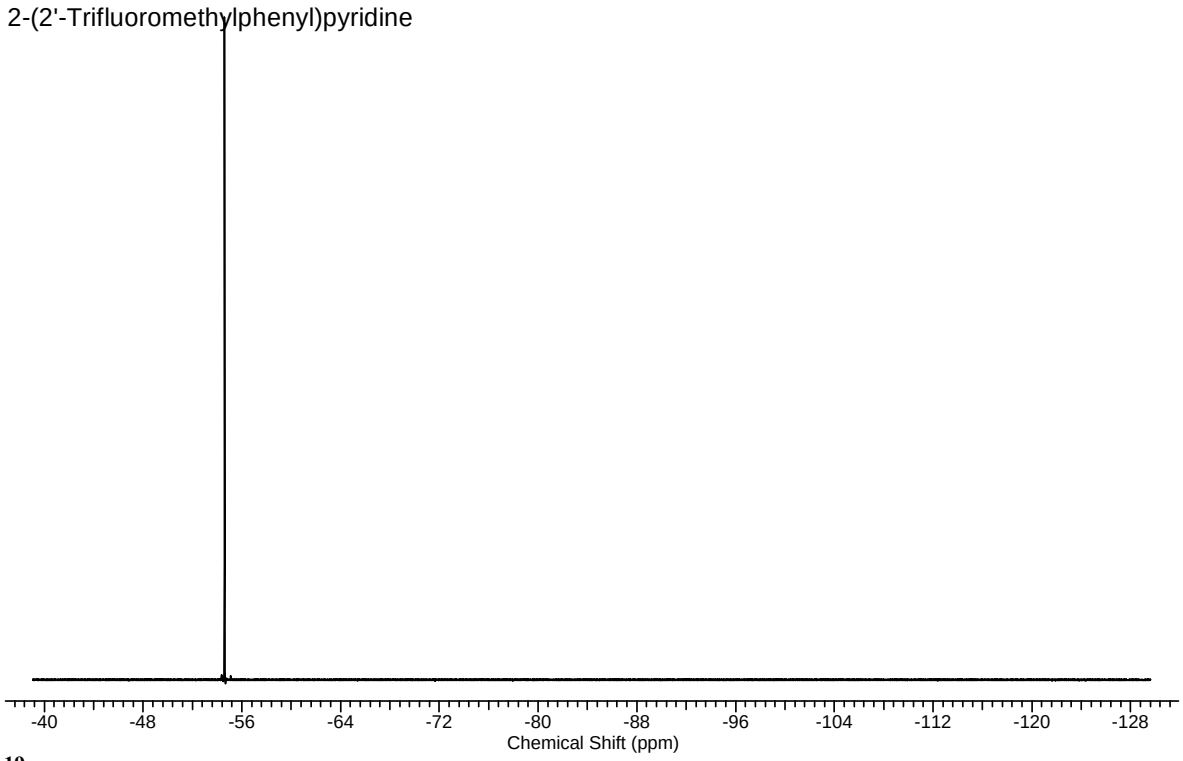

^{19}F NMR Spectrum of 2-(2′-trifluoromethylphenyl)pyridine in DMSO-d_6.

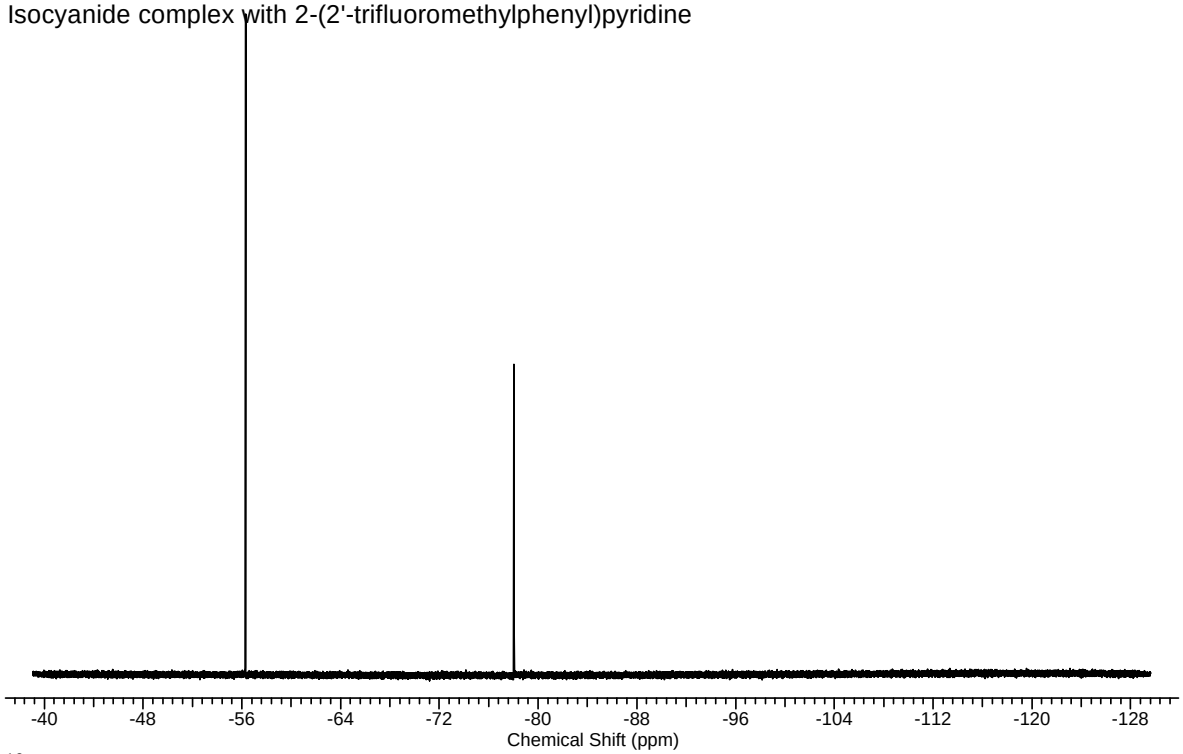

^{19}F NMR Spectrum of isocyanide complex with 2-(2′-trifluoromethylphenyl)pyridine in CD_2Cl_2.

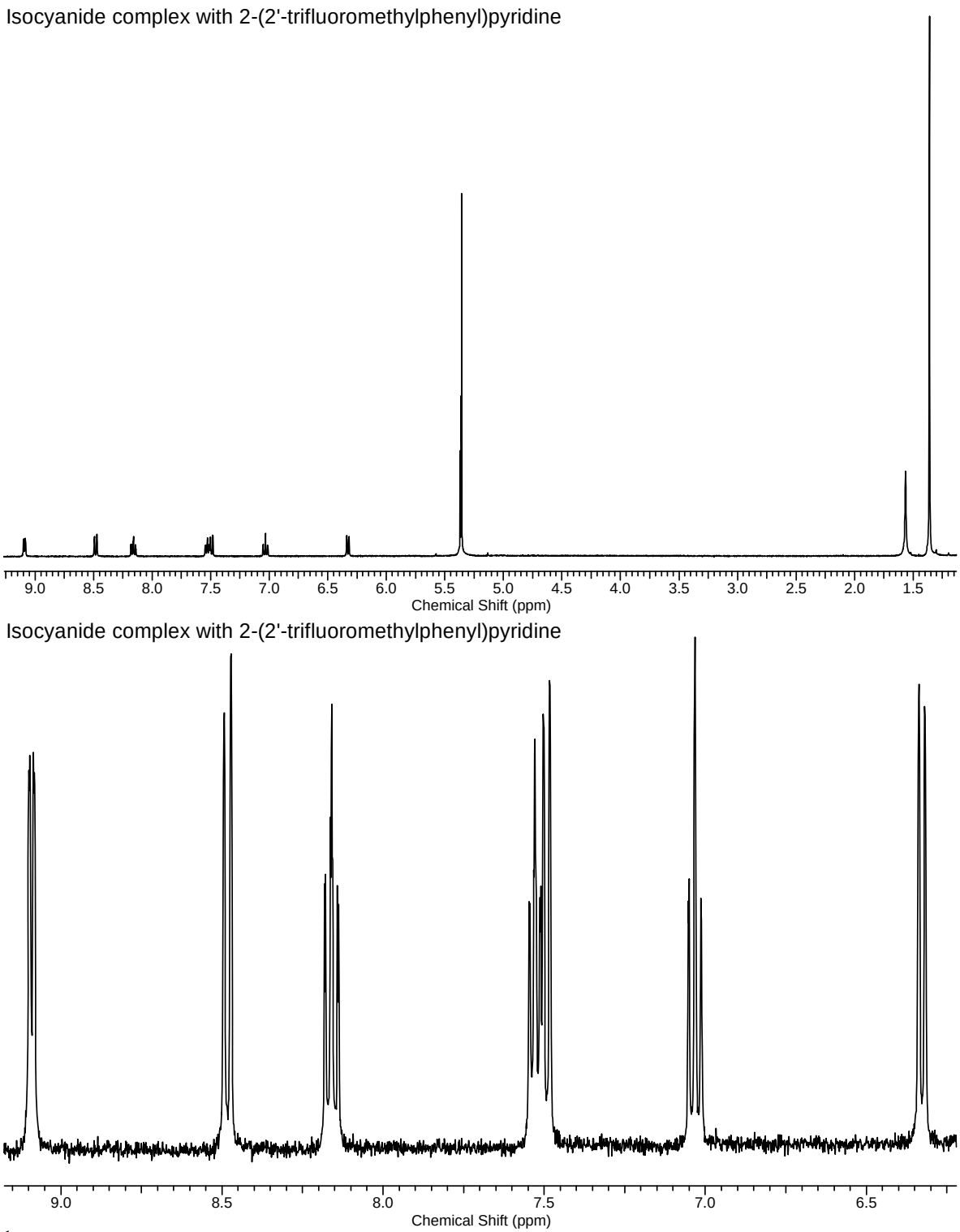

^{1}H NMR Spectrum of isocyanide complex with 2-(2′-trifluoromethylphenyl)pyridine in CD_2Cl_2 (top, complete; bottom, arom. H).

7-C. 2-(2′,4′-Bis-(trifluoromethyl)phenyl)pyridine L3, $[(L3)_2Ir(\mu\text{-}Cl)]_2$, 3

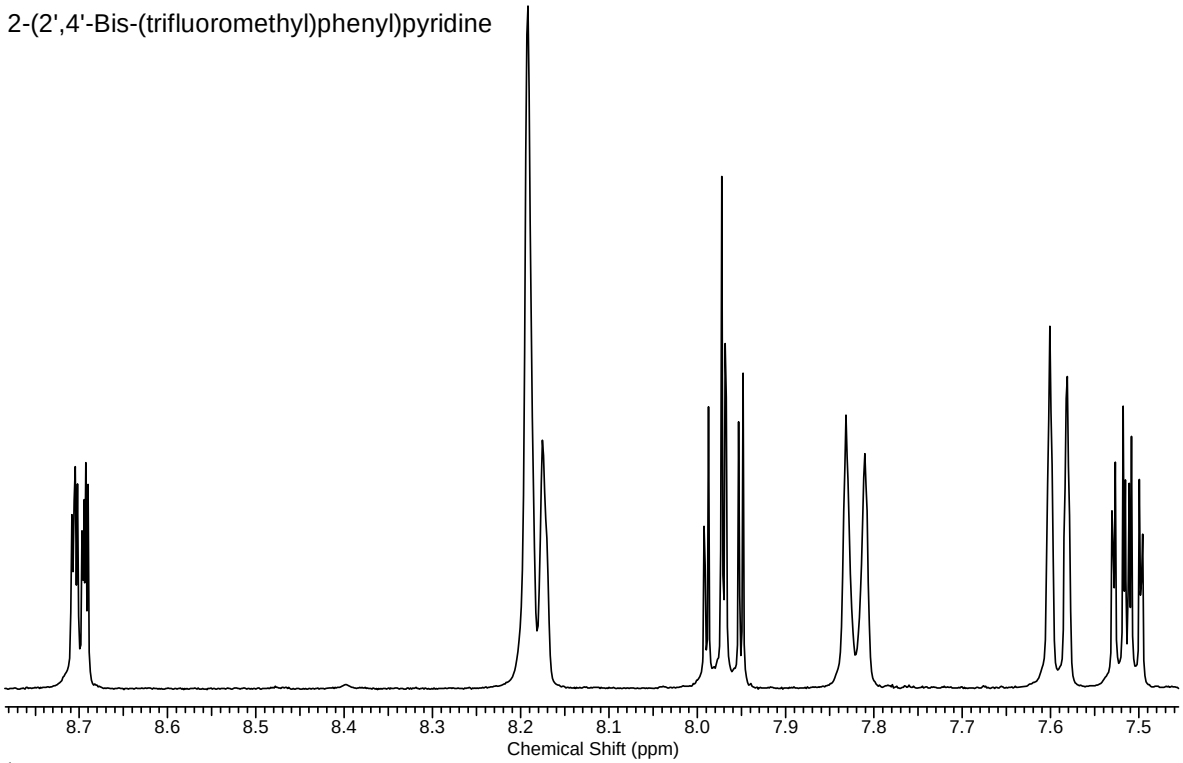

^{1}H NMR Spectrum of 2-(2′,4′-bis-(trifluoromethyl)phenyl)pyridine in DMSO-d_6.

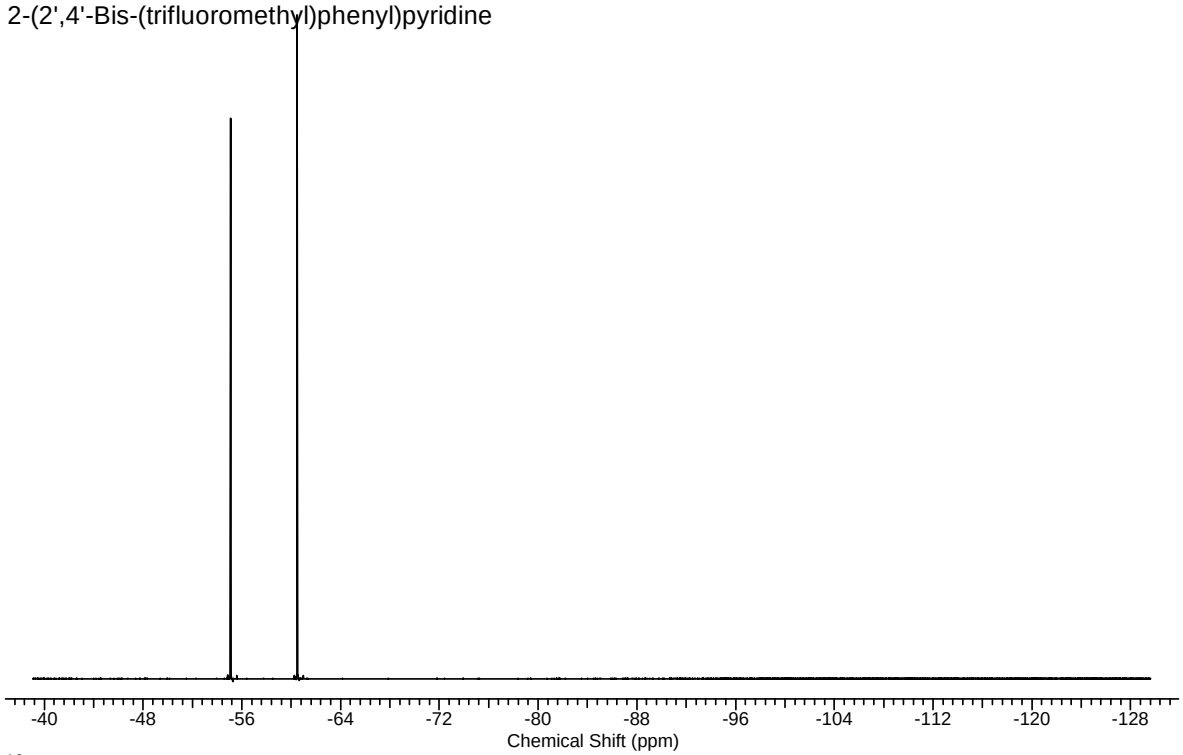

^{19}F NMR Spectrum of 2-(2′,4′-bis-(trifluoromethyl)phenyl)pyridine in DMSO-d_6.

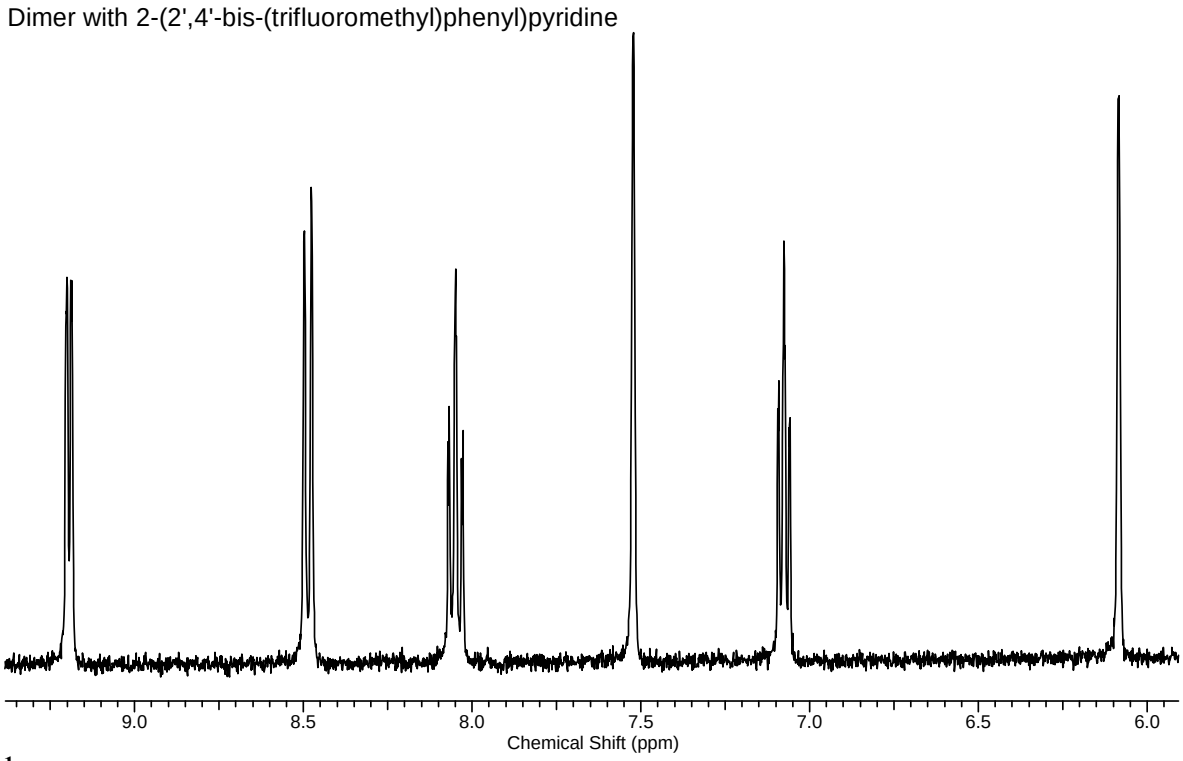

^{1}H NMR Spectrum of $[(C^N)_2Ir(\mu\text{-}Cl)]_2$ for 2-(2′,4′-bis-(trifluoromethyl)phenyl)pyridine in CD_2Cl_2.

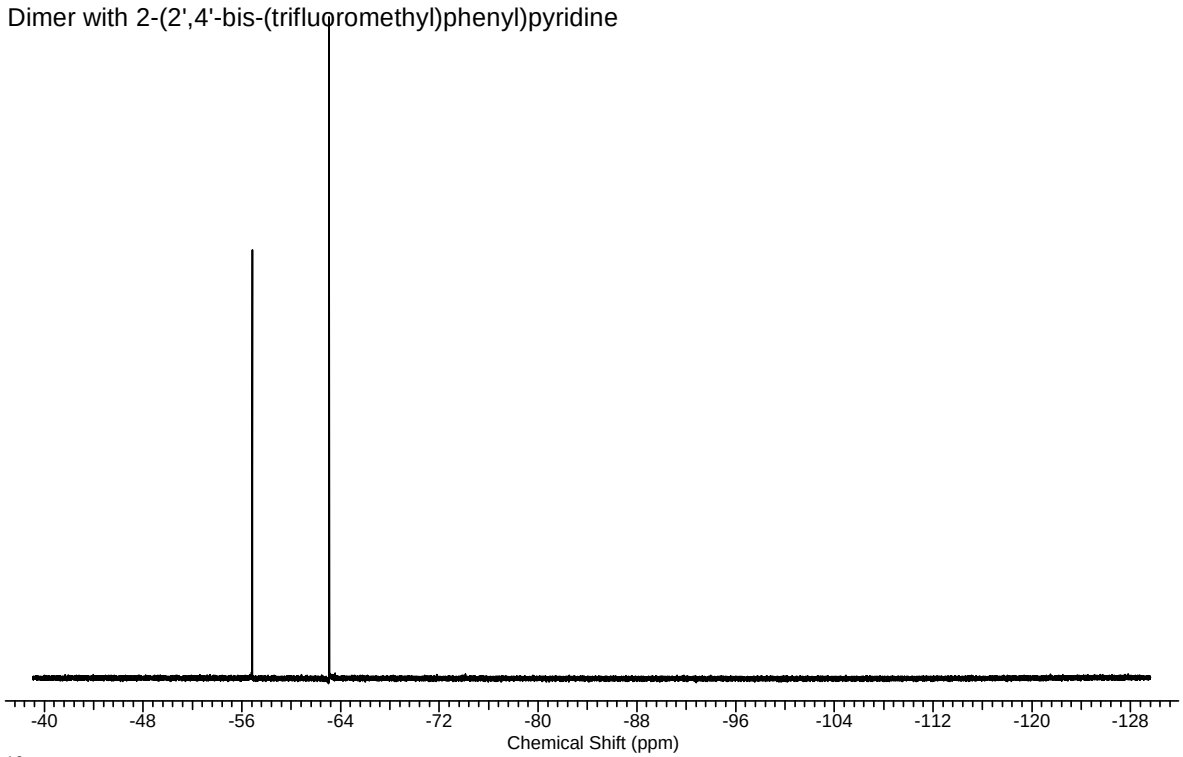

^{19}F NMR Spectrum of $[(C^N)_2Ir(\mu\text{-}Cl)]_2$ for 2-(2′,4′-bis-(trifluoromethyl)phenyl)pyridine in CD_2Cl_2.

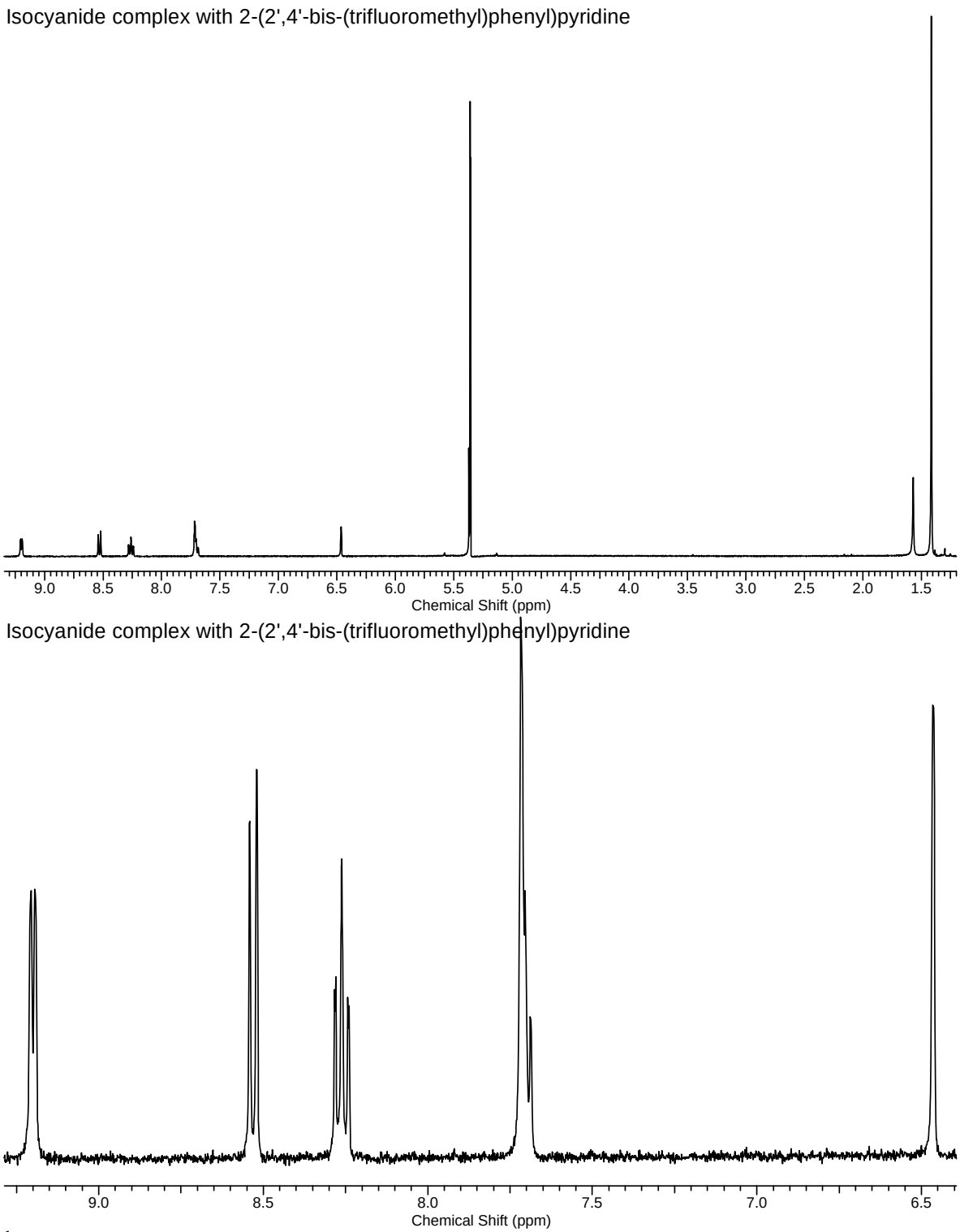

^{1}H NMR Spectrum of isocyanide complex with 2-(2′,4′-bis-(trifluoromethyl)phenyl)pyridine in CD_2Cl_2 (top, complete; bottom, arom. H).

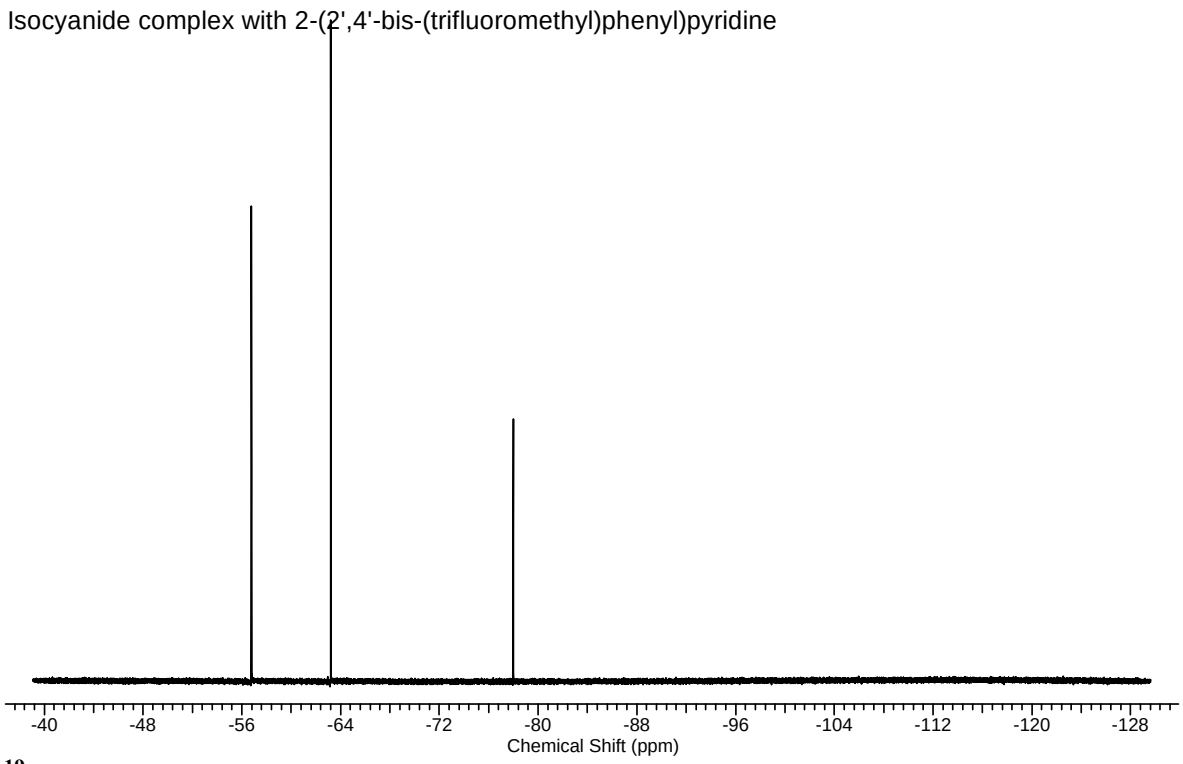

^{19}F NMR Spectrum of isocyanide complex with 2-(2′,4′-bis-(trifluoromethyl)phenyl)pyridine in CD_2Cl_2.

7-D. 2-(3′-Trifluoromethylphenyl)pyridine L4, $[(L4)_2Ir(\mu\text{-}Cl)]_2$, 4

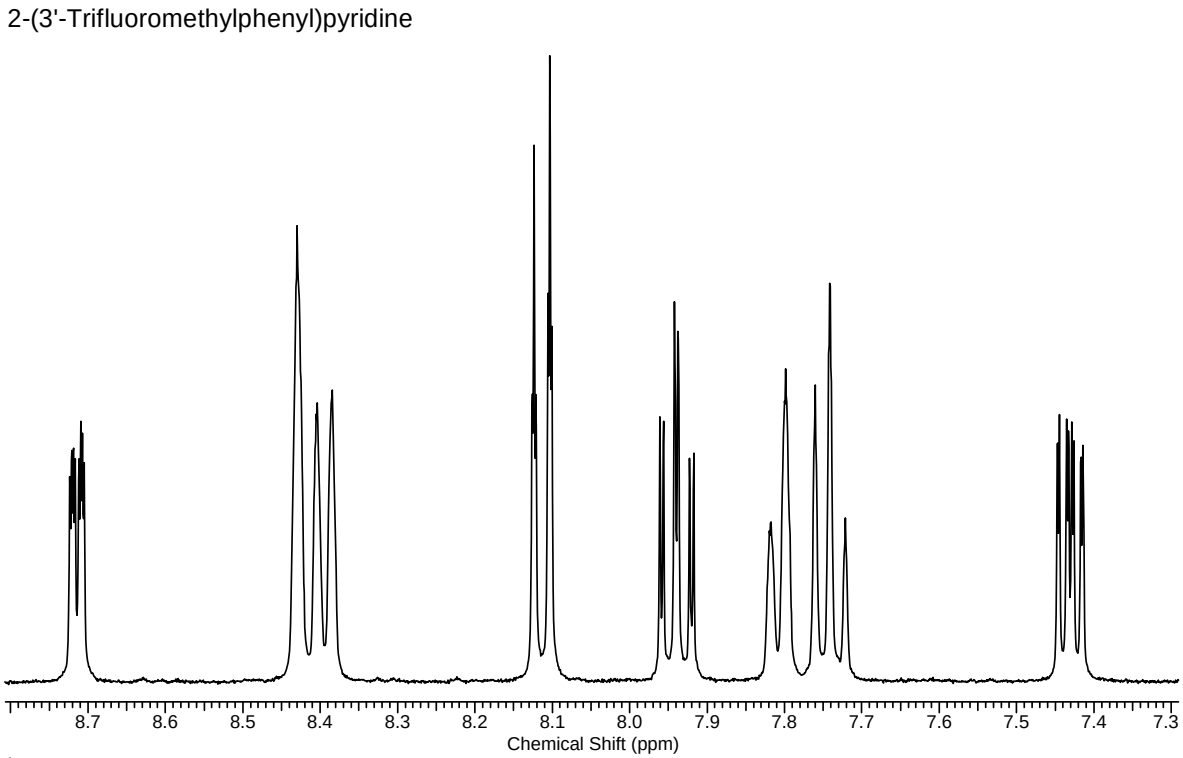

^{1}H NMR Spectrum of 2-(3′-trifluoromethylphenyl)pyridine in DMSO-d_6.

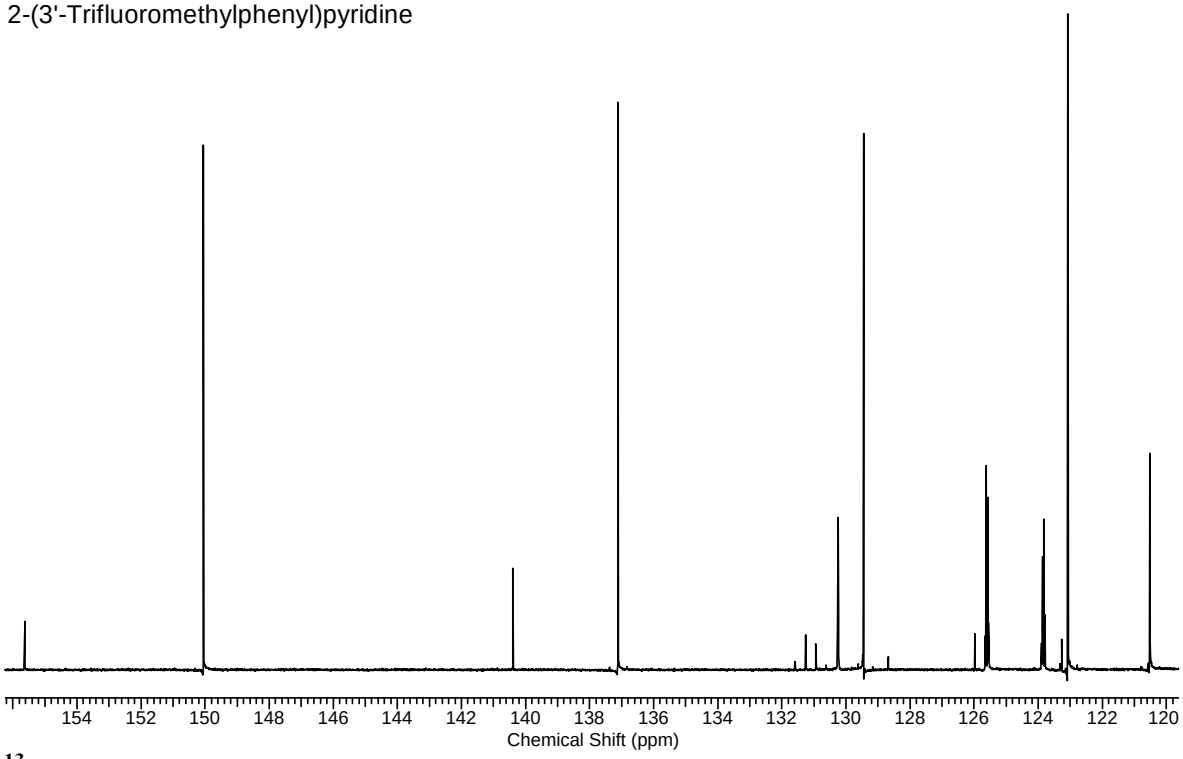

^{13}C NMR Spectrum of 2-(3′-trifluoromethylphenyl)pyridine in CD_2Cl_2.

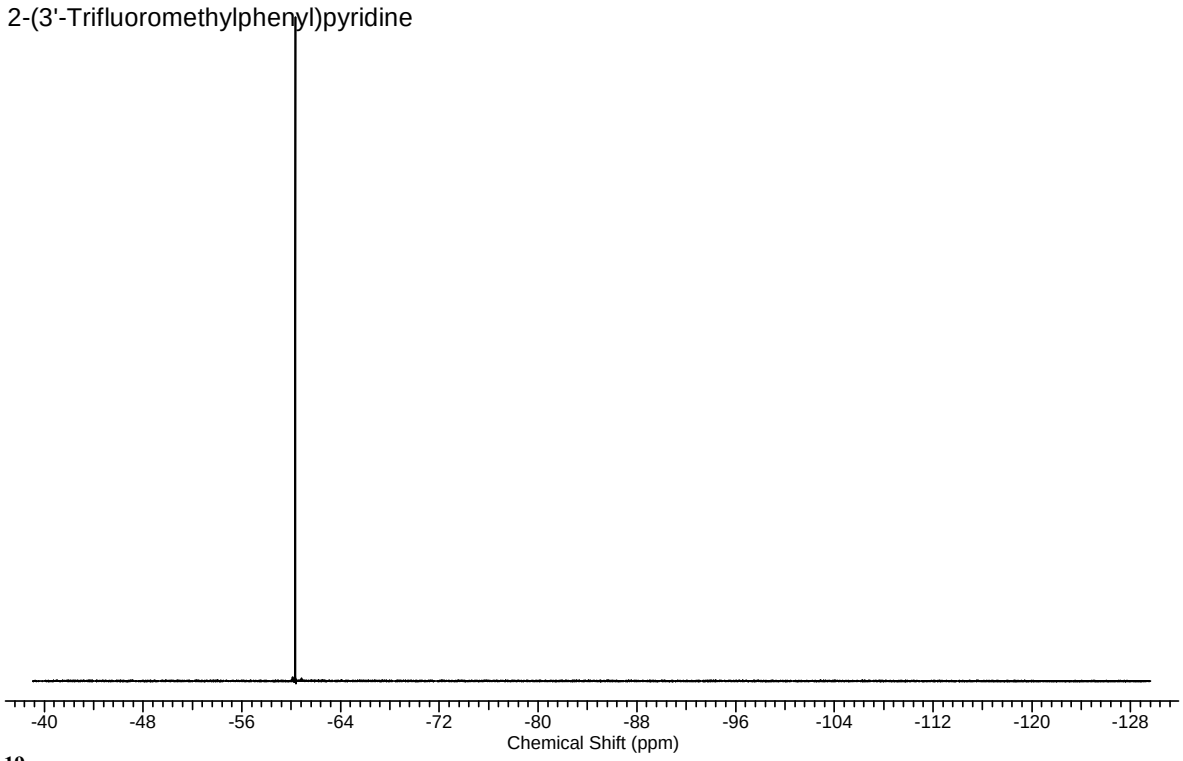

^{19}F NMR Spectrum of 2-(3′-trifluoromethylphenyl)pyridine in DMSO-d_6.

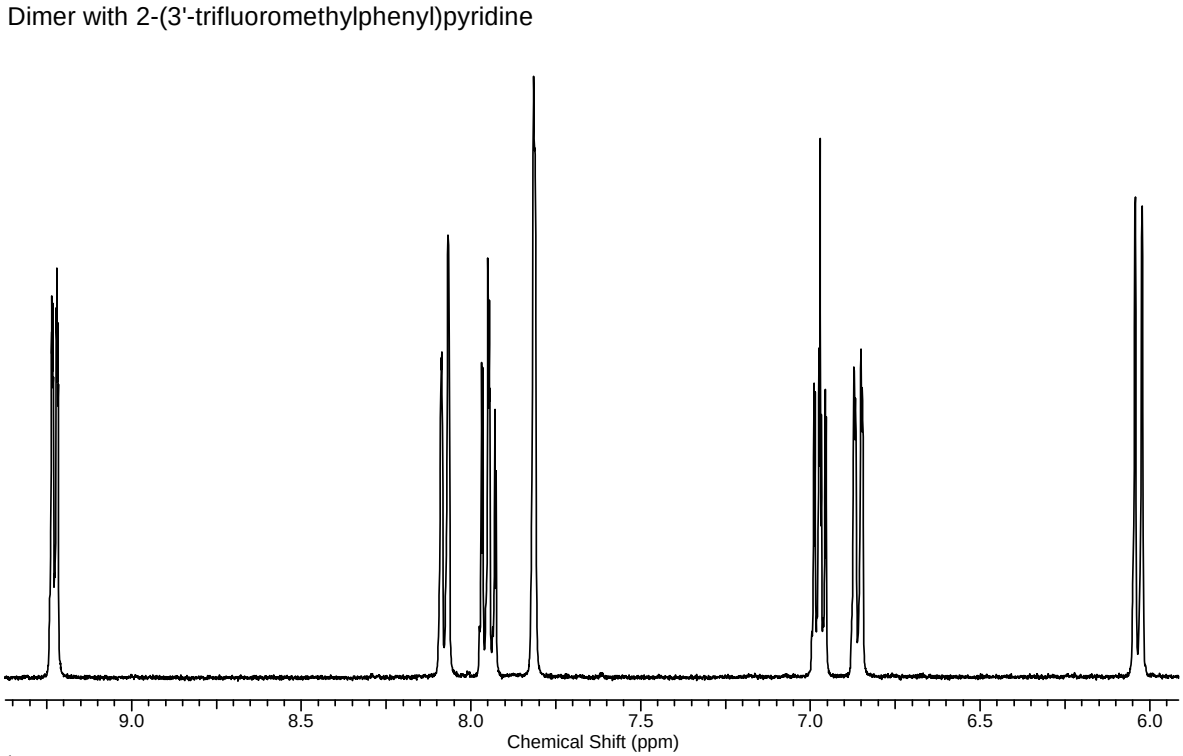

^{1}H NMR Spectrum of $[(C\hat{}N)_2Ir(\mu\text{-}Cl)]_2$ for 2-(3′-trifluoromethylphenyl)pyridine in CD_2Cl_2.

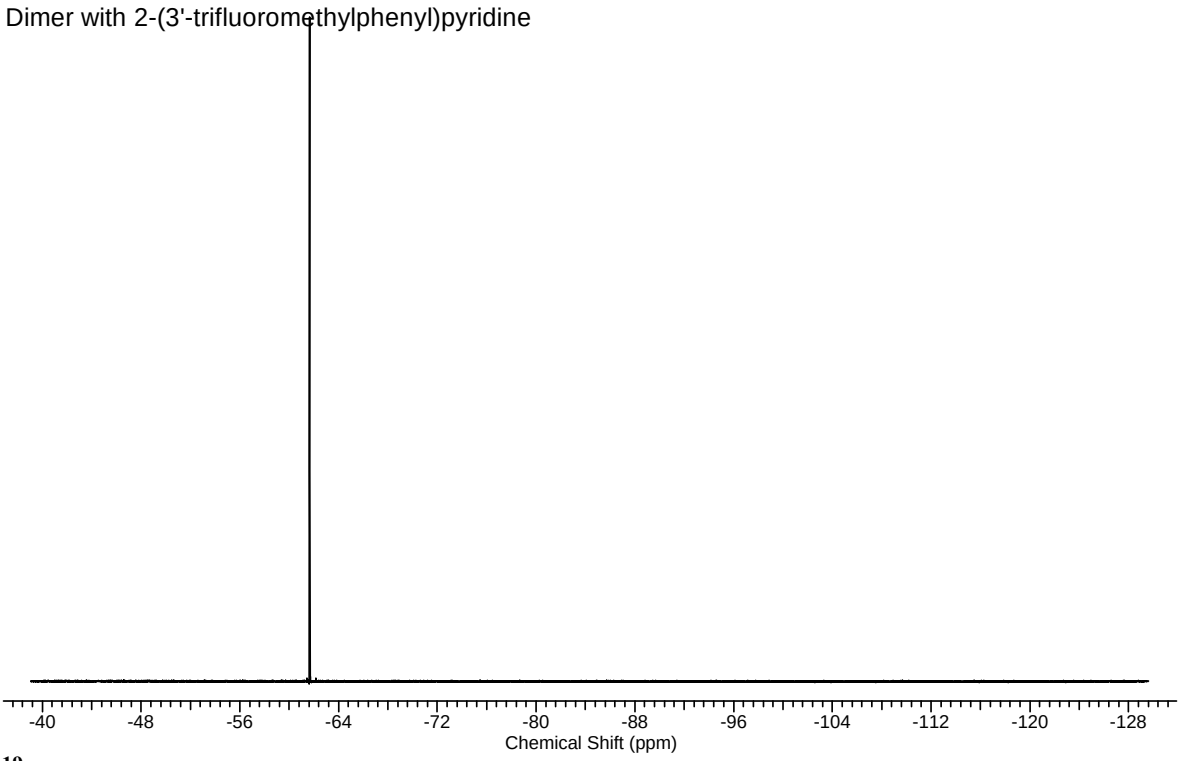

^{19}F NMR Spectrum of $[(C^N)_2Ir(\mu\text{-}Cl)]_2$ for 2-(3′-trifluoromethylphenyl)pyridine in CD_2Cl_2.

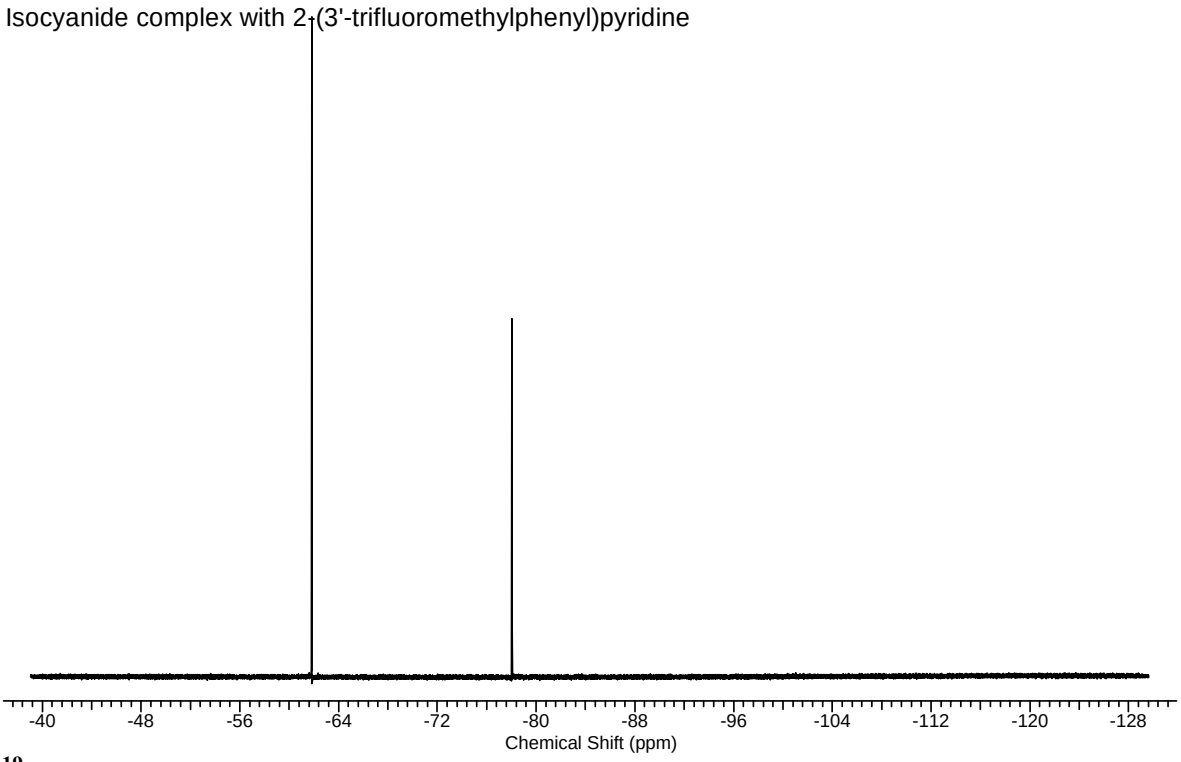

^{19}F NMR Spectrum of isocyanide complex with 2-(3′-trifluoromethylphenyl)pyridine in CD_2Cl_2.

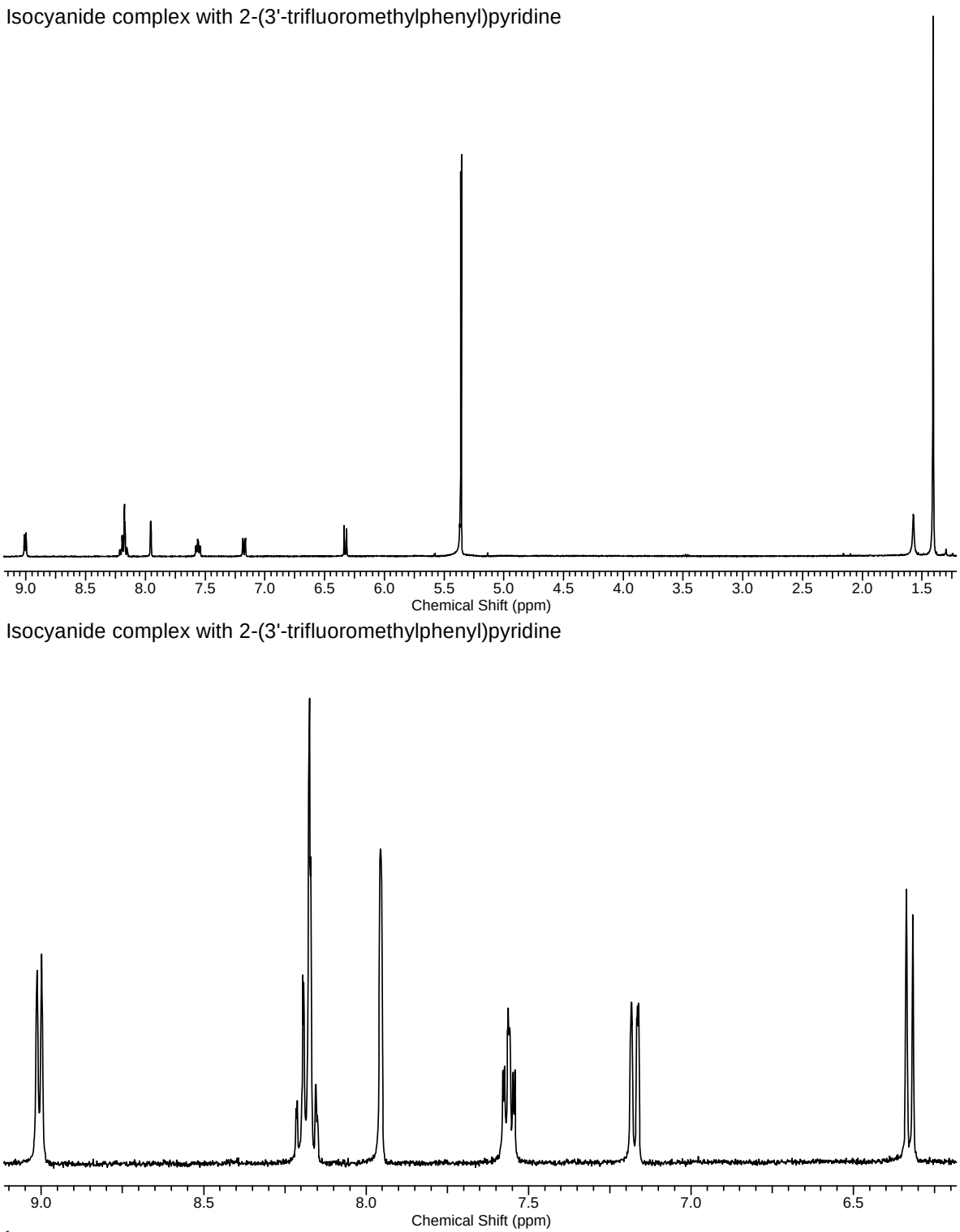

^{1}H NMR Spectrum of isocyanide complex with 2-(3′-trifluoromethylphenyl)pyridine in CD_2Cl_2 (top, complete; bottom, arom. H).

7-E. 2-(3′,5′-Bis(trifluoromethyl)phenyl)pyridine L5, $[(L5)_2Ir(\mu\text{-}Cl)]_2$, 5

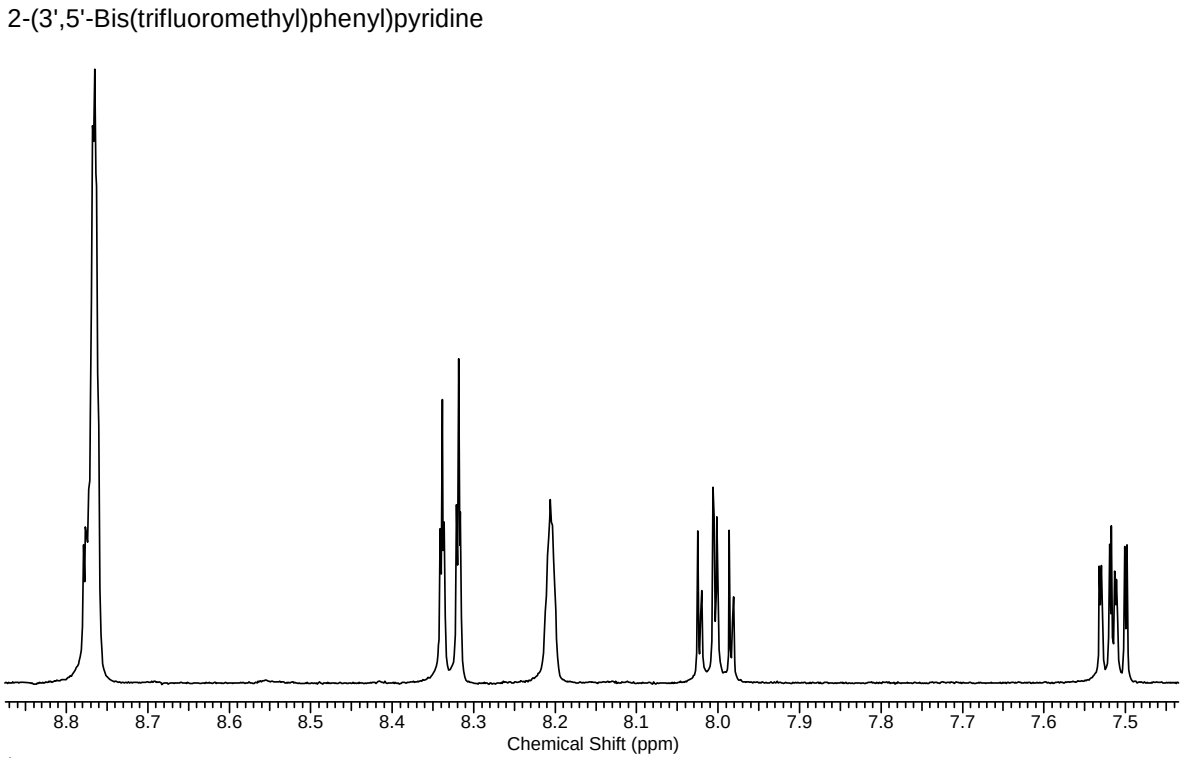

^{1}H NMR Spectrum of 2-(3′,5′-bis(trifluoromethyl)phenyl)pyridine in DMSO-d_6.

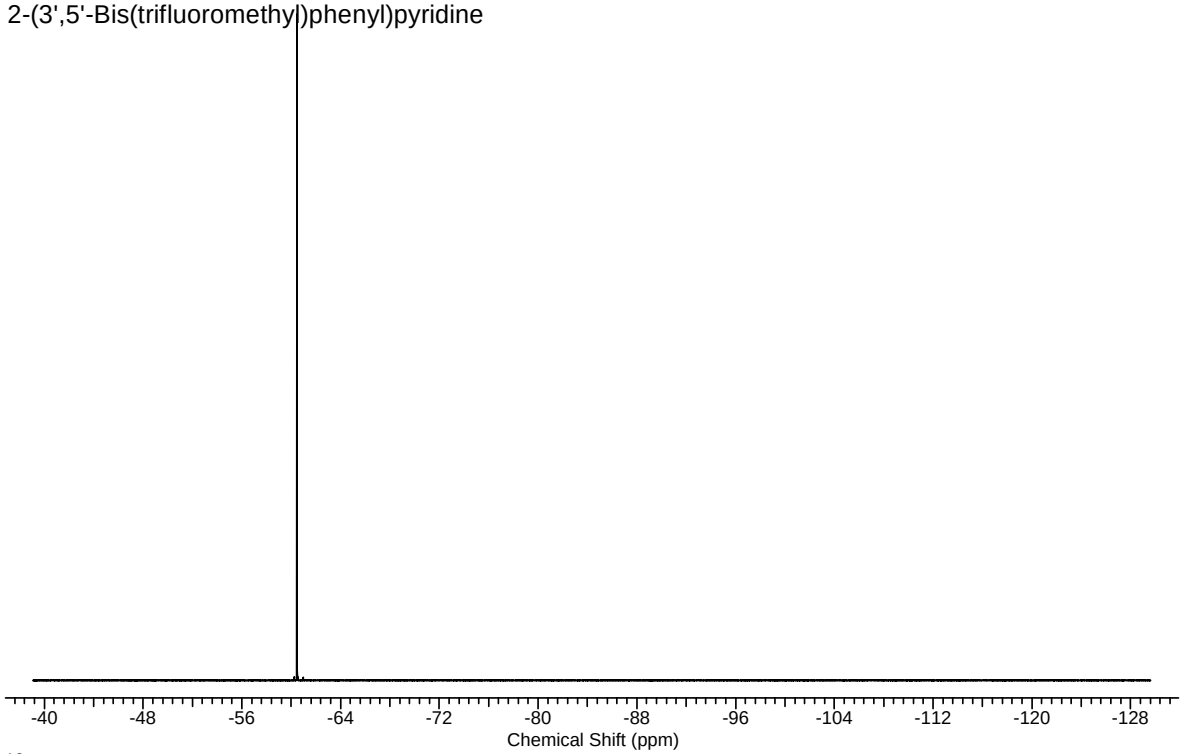

^{19}F NMR Spectrum of 2-(3′,5′-bis(trifluoromethyl)phenyl)pyridine in DMSO-d_6.

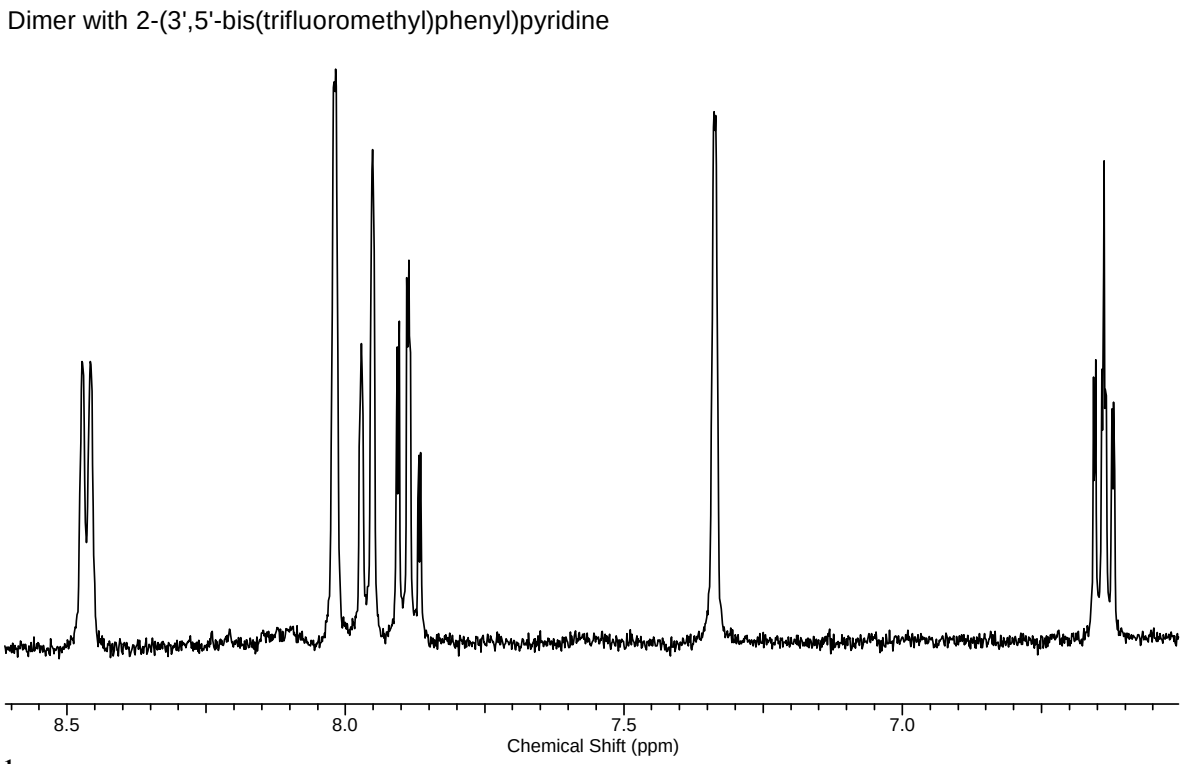

^{1}H NMR Spectrum of $[(C^N)_2Ir(\mu\text{-}Cl)]_2$ for 2-(3′,5′-bis(trifluoromethyl)phenyl)pyridine in CD_2Cl_2.

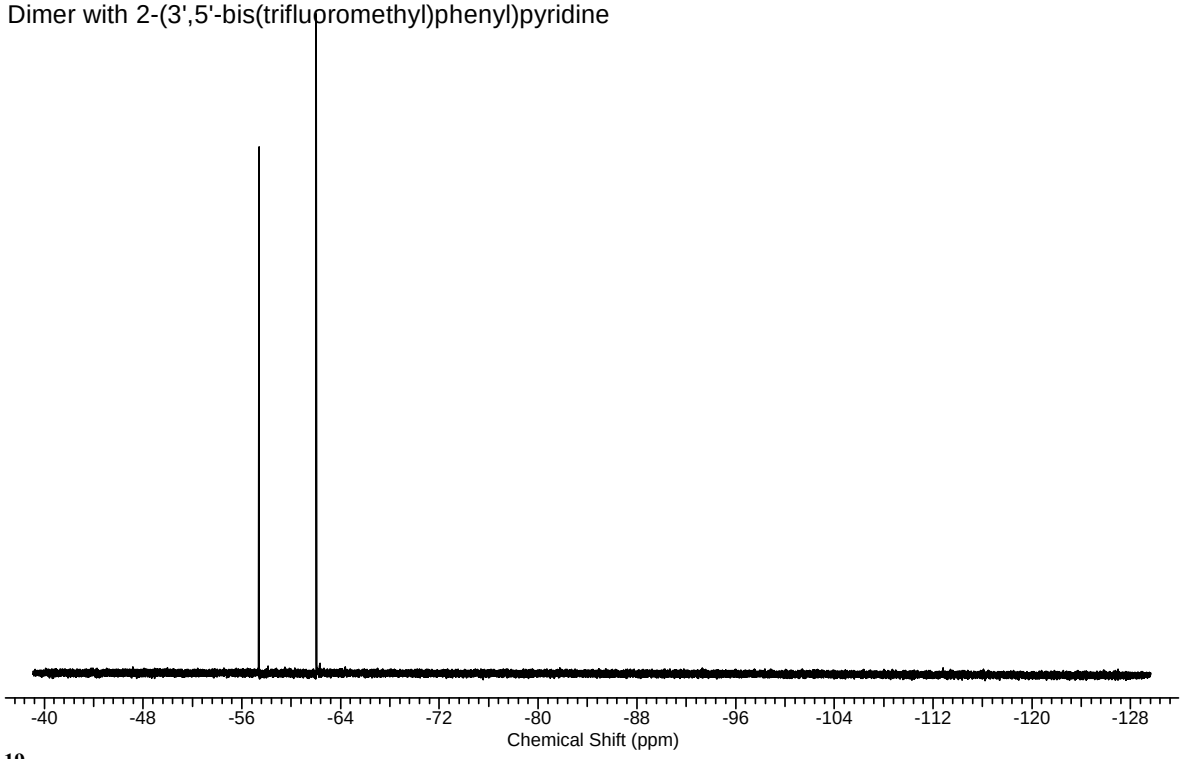

^{19}F NMR Spectrum of $[(C^N)_2Ir(\mu\text{-}Cl)]_2$ for 2-(3′,5′-bis(trifluoromethyl)phenyl)pyridine in CD_2Cl_2.

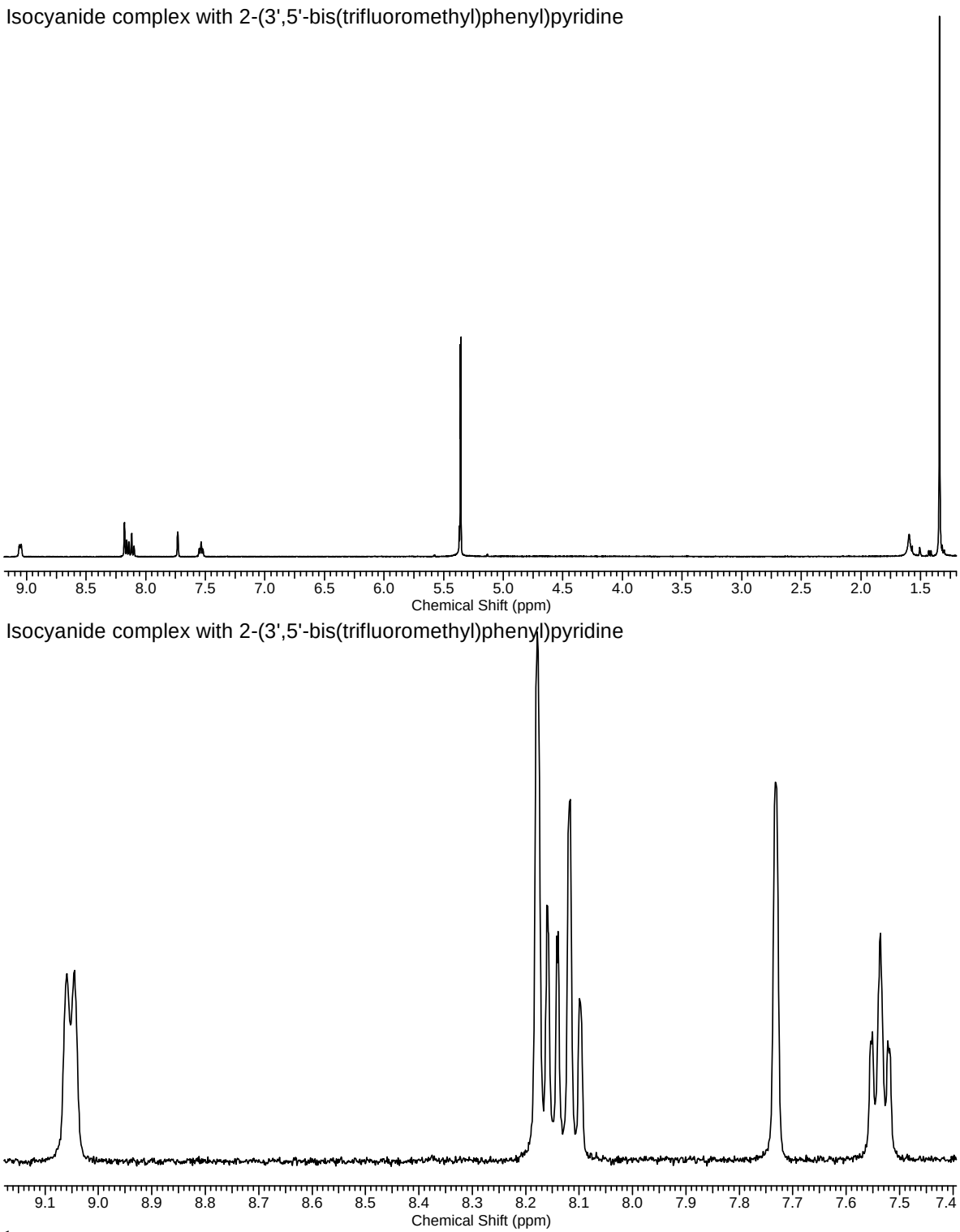

^{1}H NMR Spectrum of isocyanide complex with 2-(3′,5′-bis(trifluoromethyl)phenyl)pyridine in CD_2Cl_2 (top, complete; bottom, arom. H).

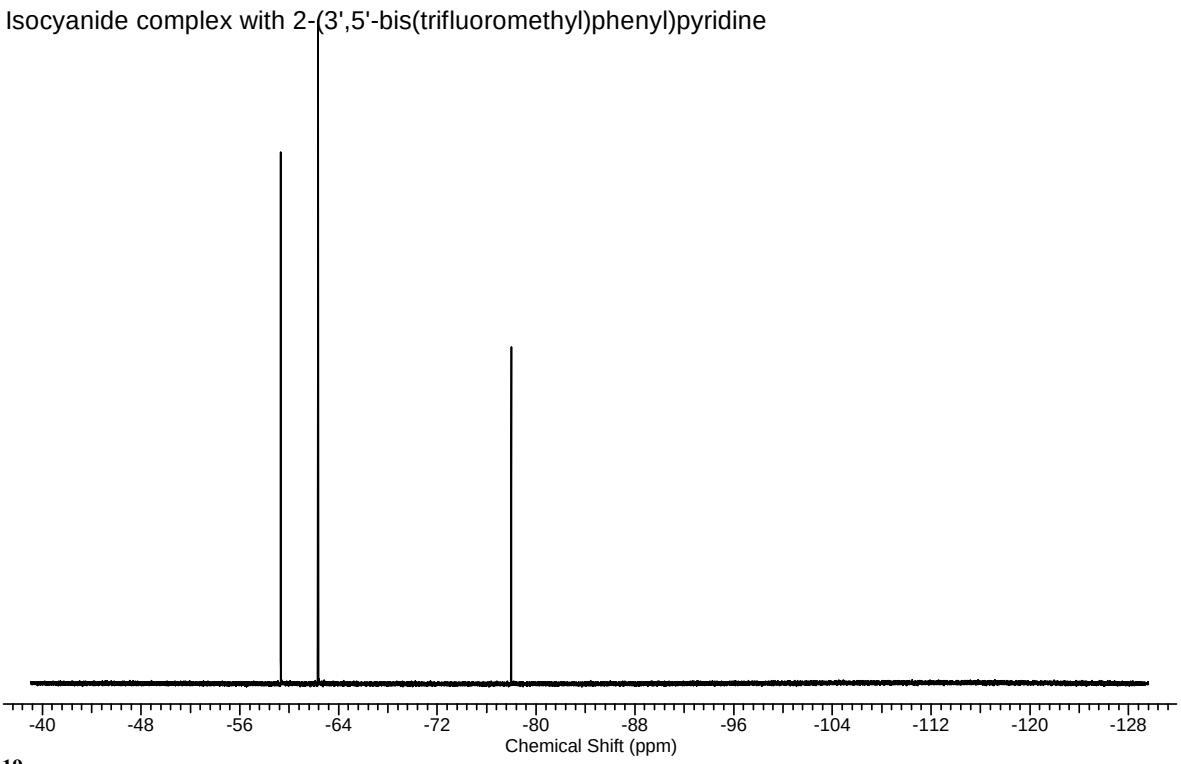

^{19}F NMR Spectrum of isocyanide complex with 2-(3′,5′-bis(trifluoromethyl)phenyl)pyridine in CD_2Cl_2.

7-F. 2-(4′-Trifluoromethoxyphenyl)pyridine L6, $[(L6)_2Ir(\mu\text{-}Cl)]_2$, 6

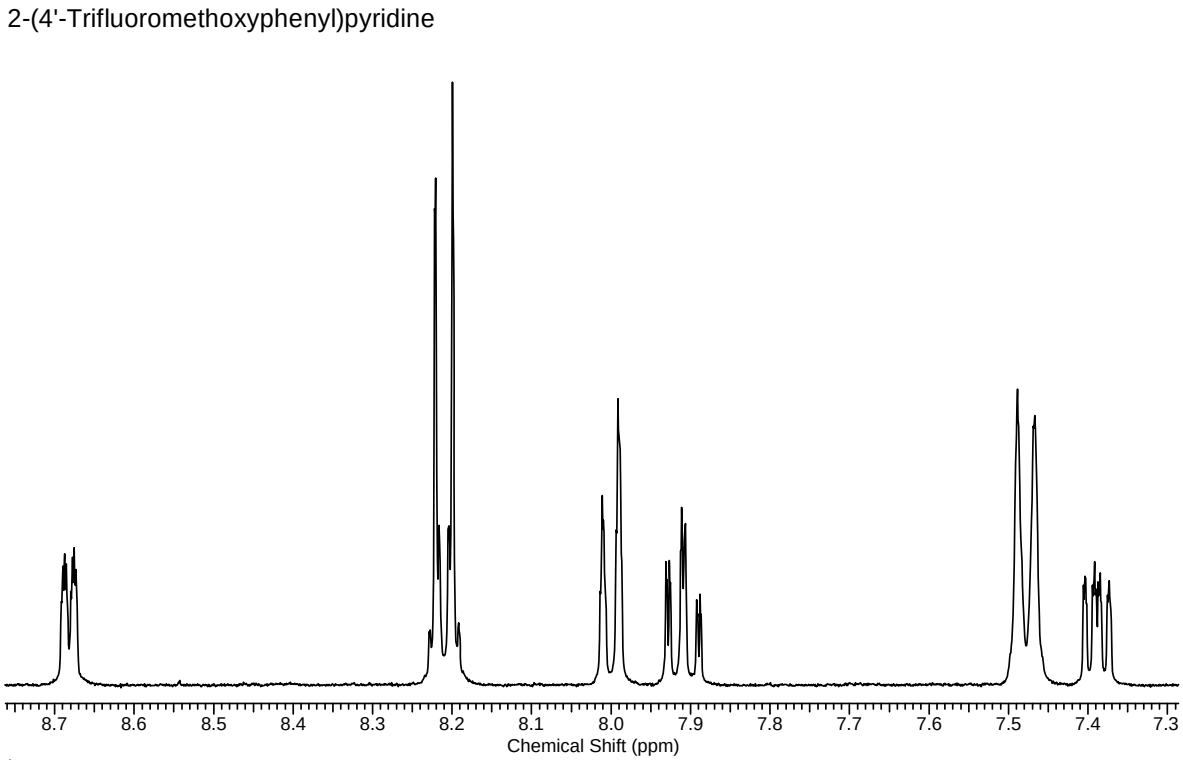

^{1}H NMR Spectrum of 2-(4′-trifluoromethoxyphenyl)pyridine in DMSO-d_6.

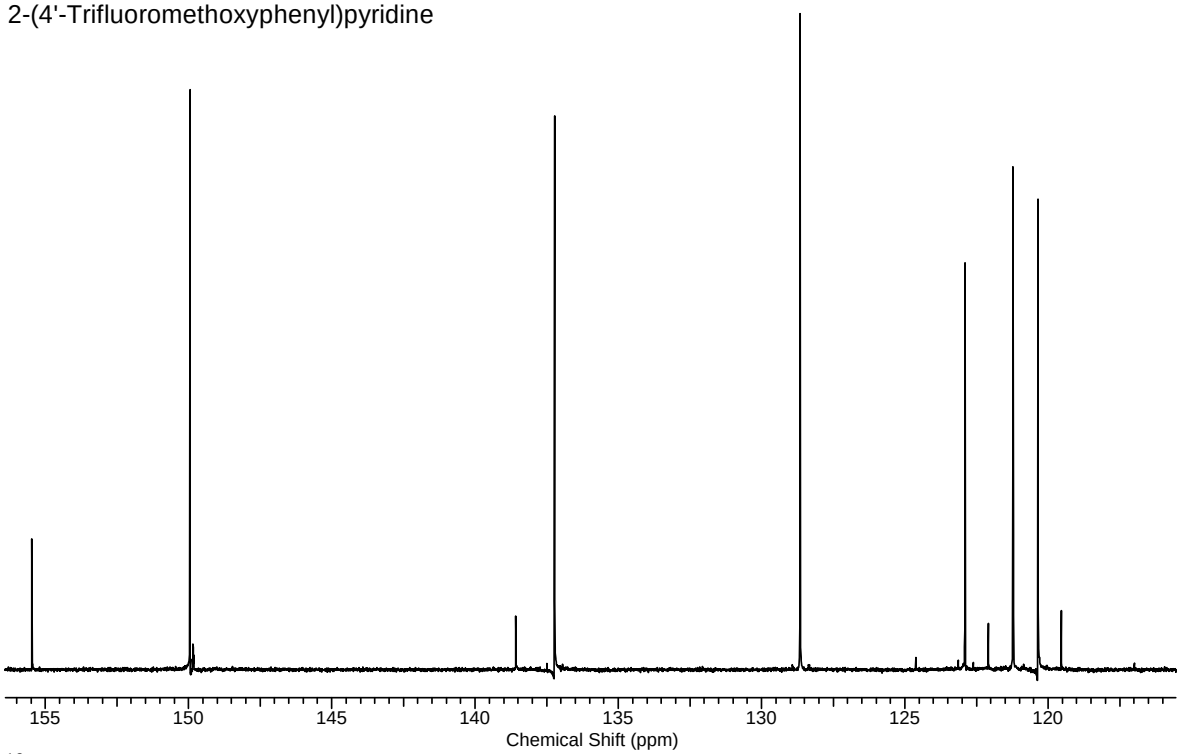

^{13}C NMR Spectrum of 2-(4′-trifluoromethoxyphenyl)pyridine in acetone-d_6.

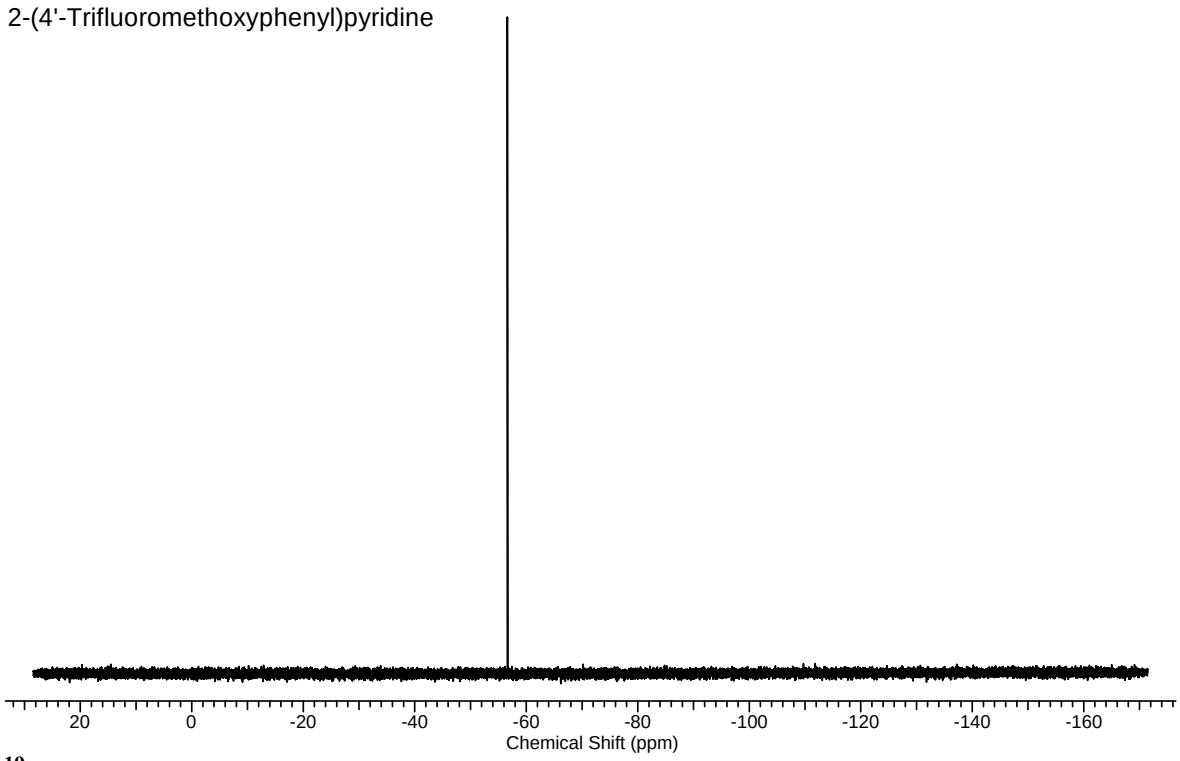

^{19}F NMR Spectrum of 2-(4′-trifluoromethoxyphenyl)pyridine in DMSO-d_6.

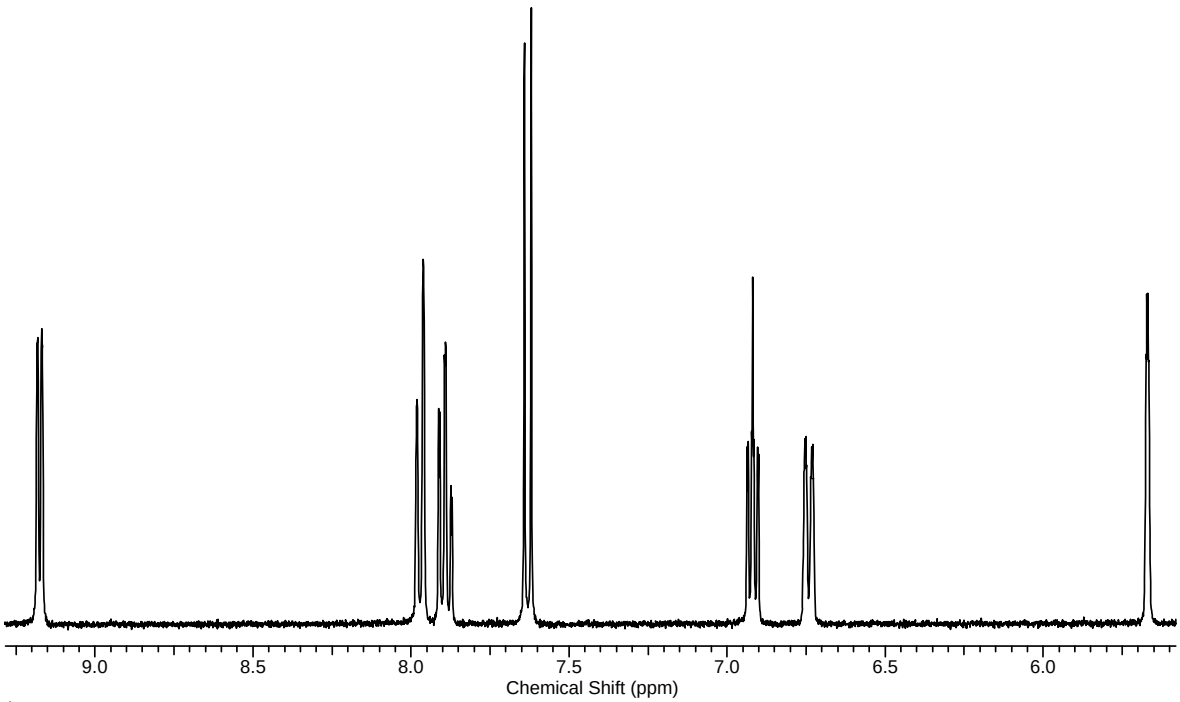

^{1}H NMR Spectrum of $[(C\hat{}N)_2Ir(\mu\text{-}Cl)]_2$ for 2-(4′-trifluoromethoxyphenyl)pyridine in CD_2Cl_2.

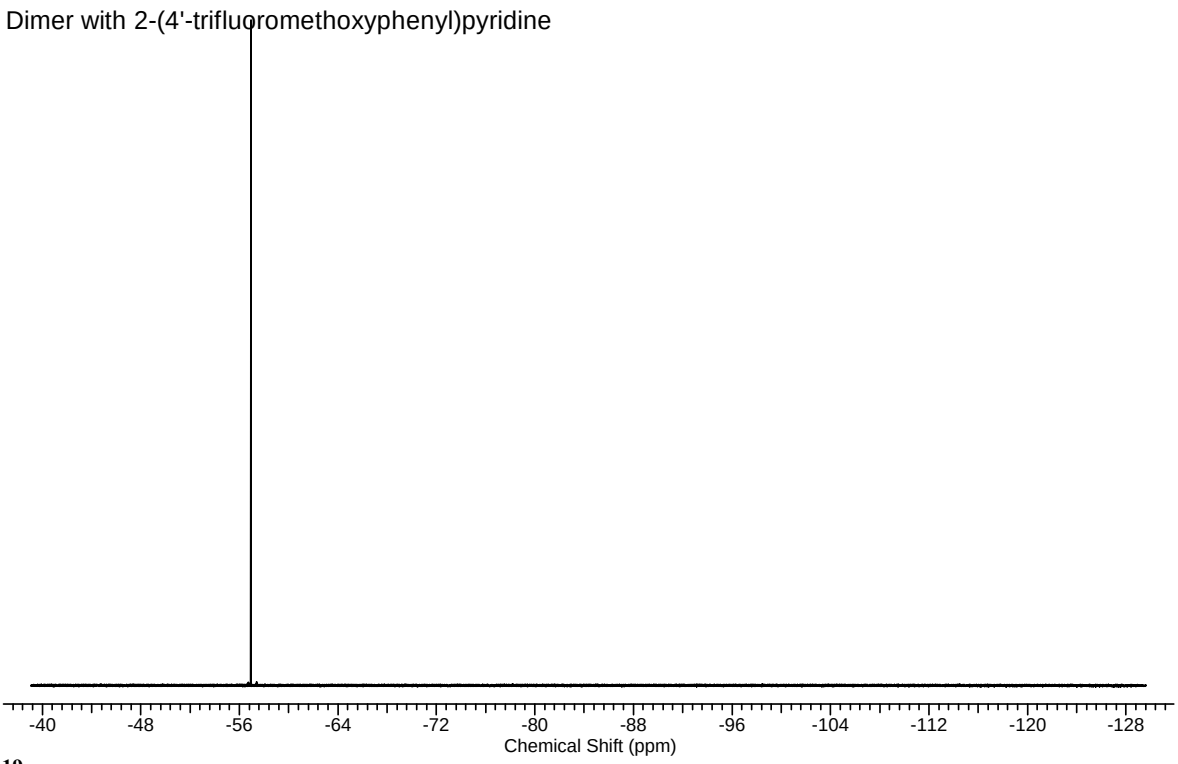

^{19}F NMR Spectrum of $[(C\hat{}N)_2Ir(\mu\text{-}Cl)]_2$ for 2-(4′-trifluoromethoxyphenyl)pyridine in CD_2Cl_2.

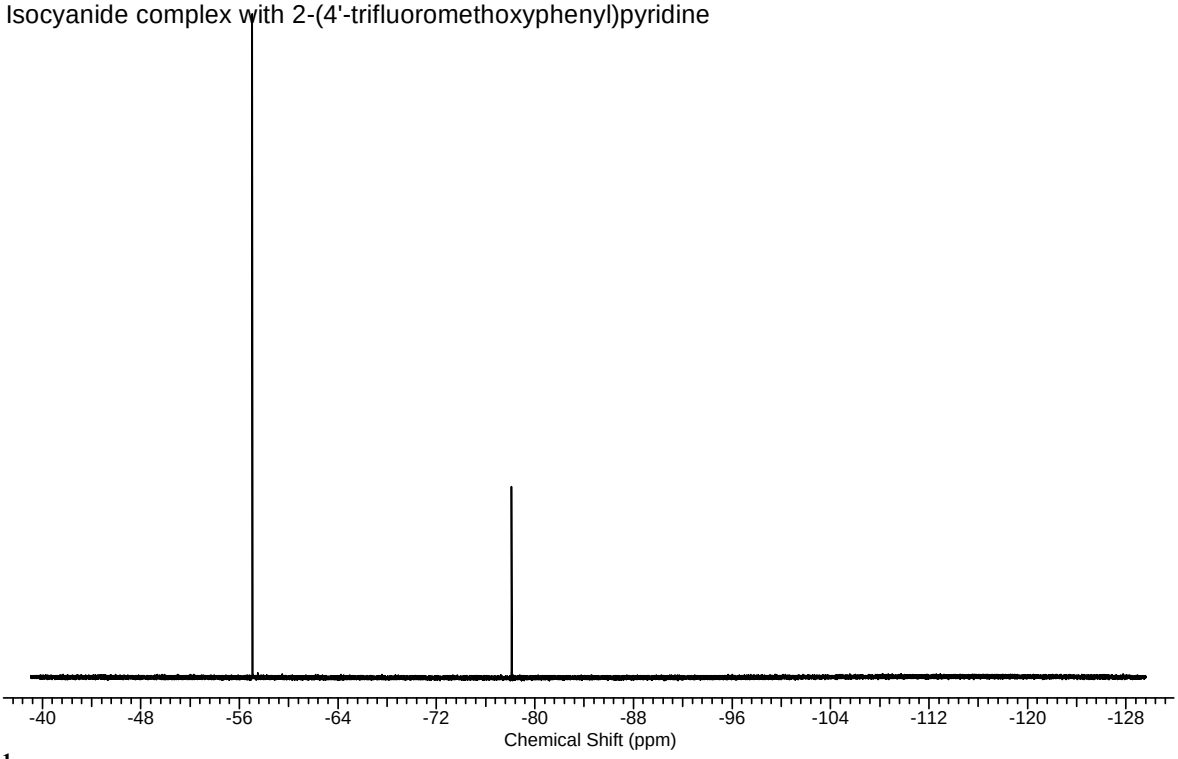

^{1}H NMR Spectrum of isocyanide complex with 2-(4′-trifluoromethoxyphenyl)pyridine in CD_2Cl_2 (top, complete; bottom, arom. H).

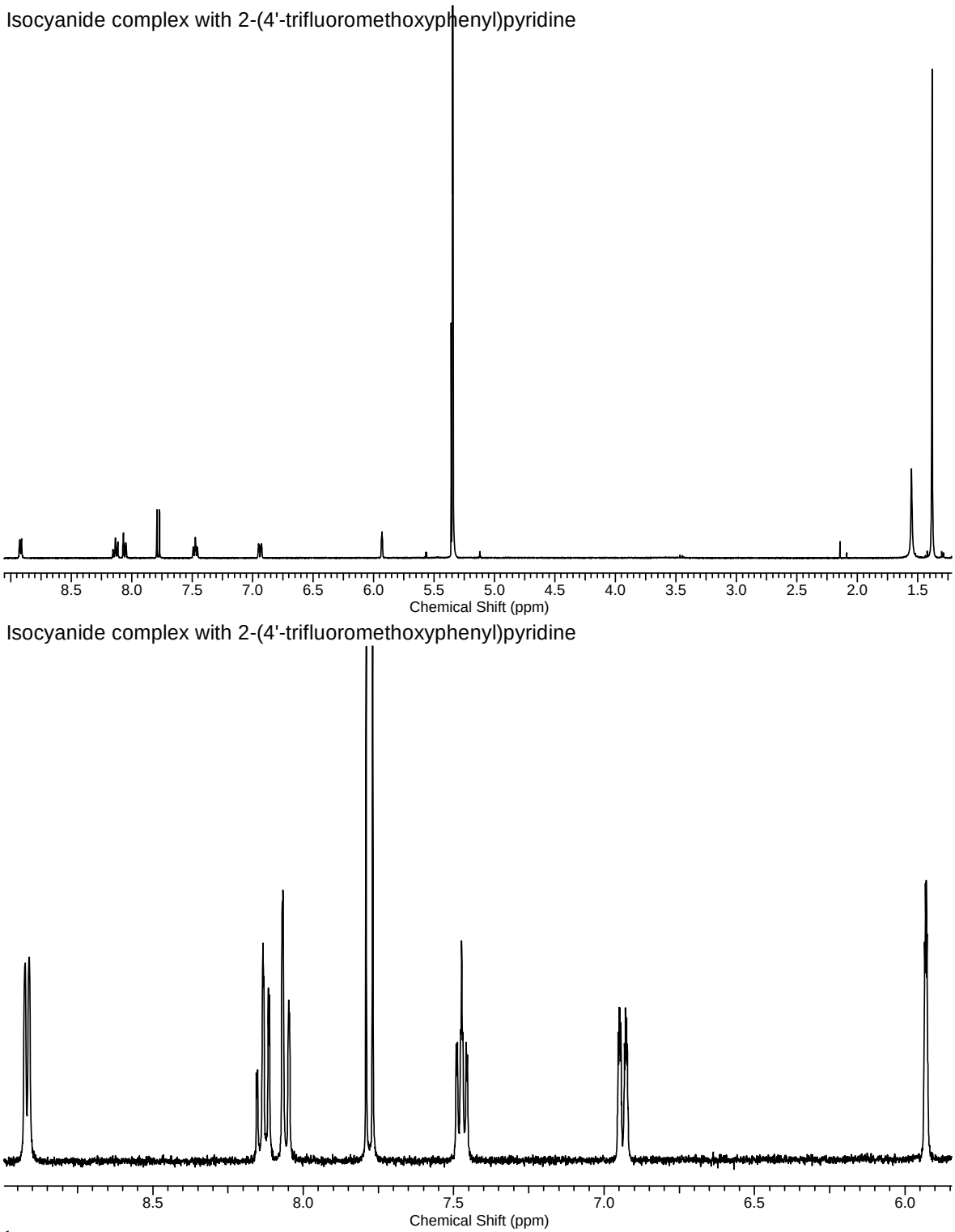

^{1}H NMR Spectrum of isocyanide complex with 2-(4′-trifluoromethoxyphenyl)pyridine in CD_2Cl_2 (top, complete; bottom, arom. H).

7-G. 2-(2′-Trifluoromethoxyphenyl)pyridine L7, $[(L7)_2Ir(\mu\text{-}Cl)]_2$, 7

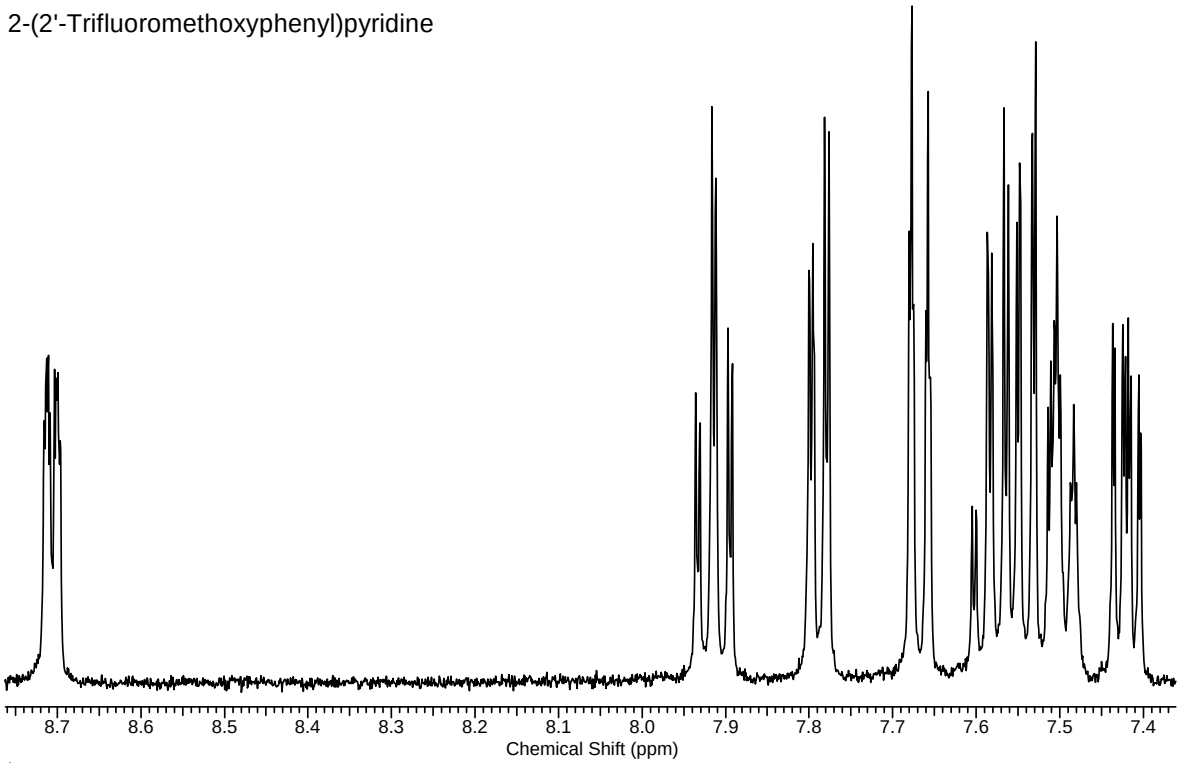

^{1}H NMR Spectrum of 2-(2′-trifluoromethoxyphenyl)pyridine in DMSO-d_6.

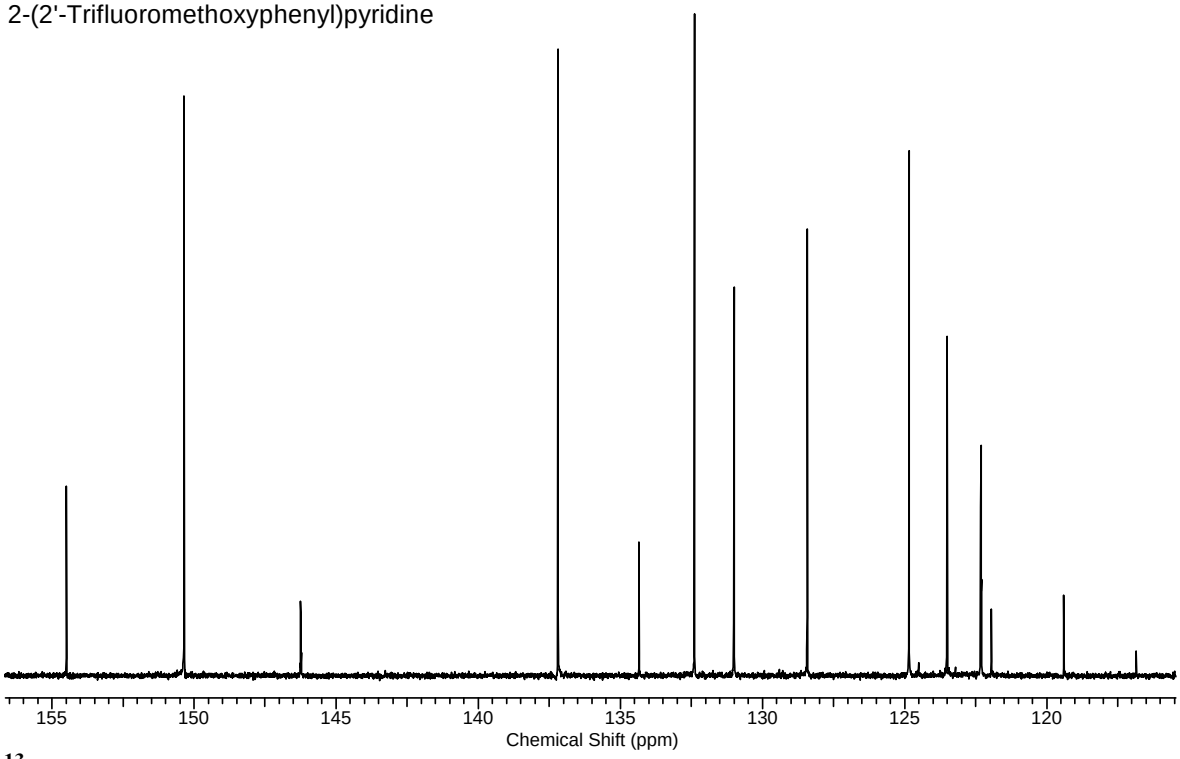

^{13}C NMR Spectrum of 2-(2′-trifluoromethoxyphenyl)pyridine in DMSO-d_6.

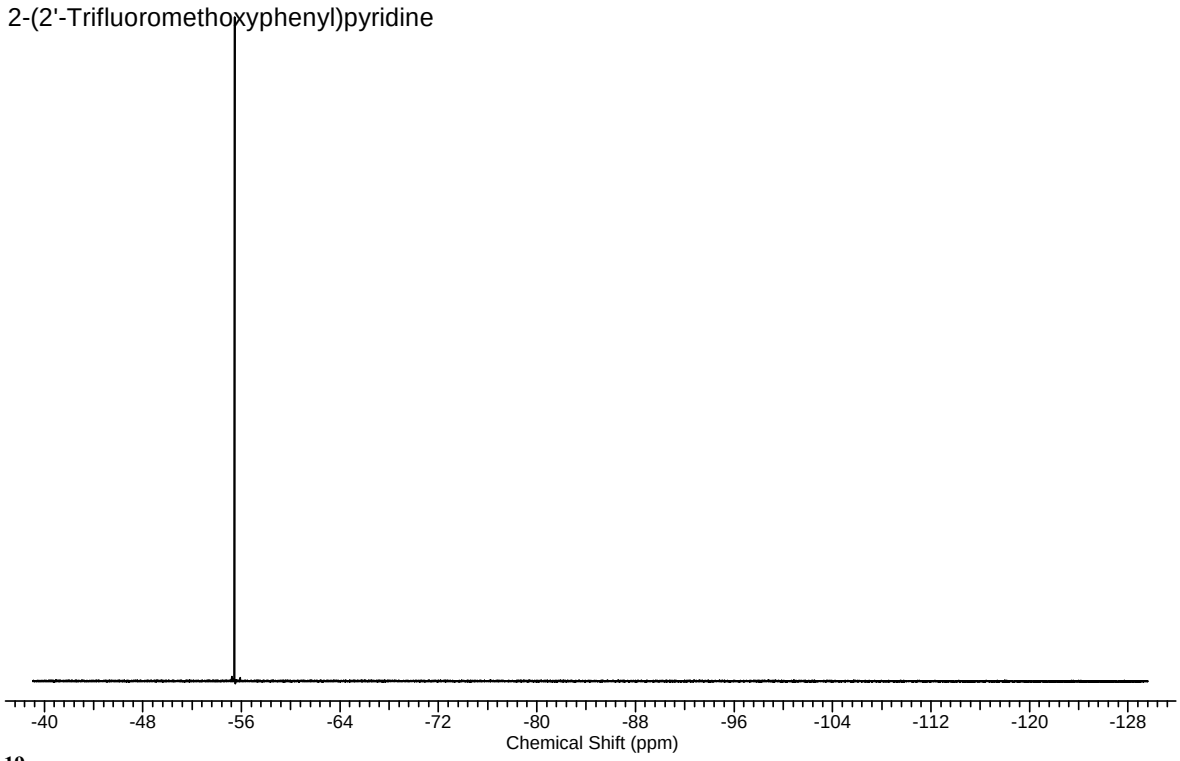

^{19}F NMR Spectrum of 2-(2′-trifluoromethoxyphenyl)pyridine in DMSO-d_6.

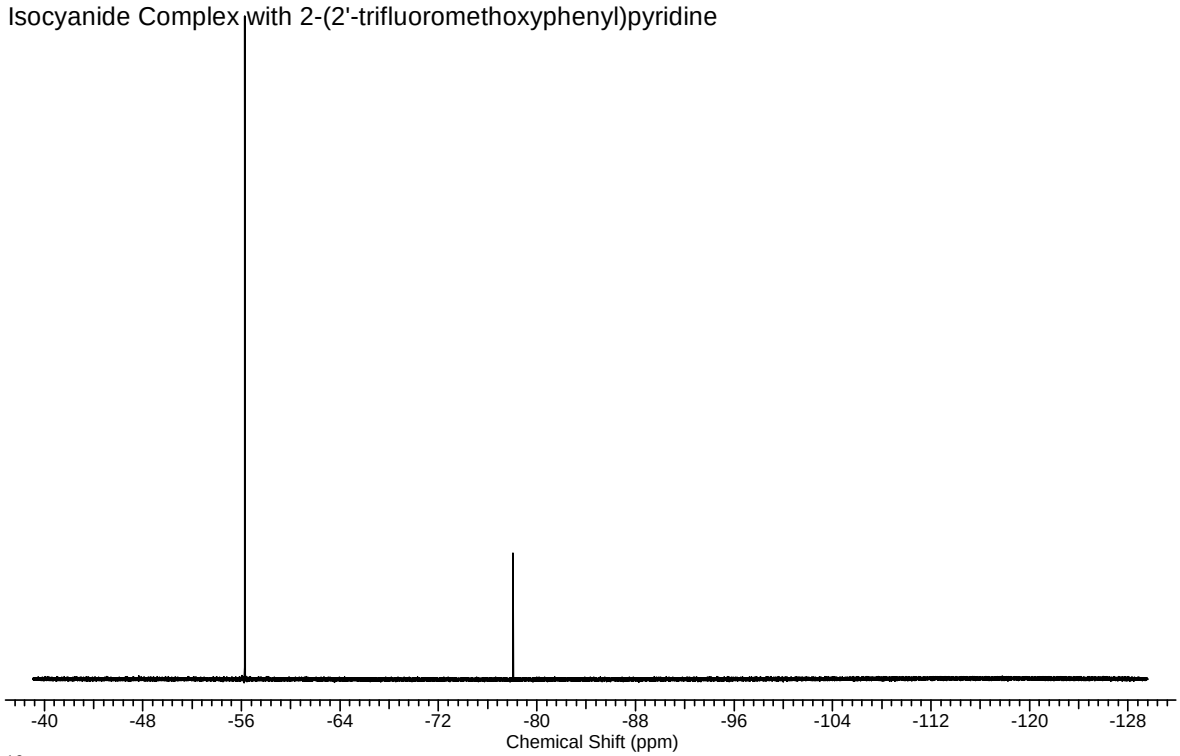

^{19}F NMR Spectrum of isocyanide complex with 2-(2′-trifluoromethoxyphenyl)pyridine in CD_2Cl_2.

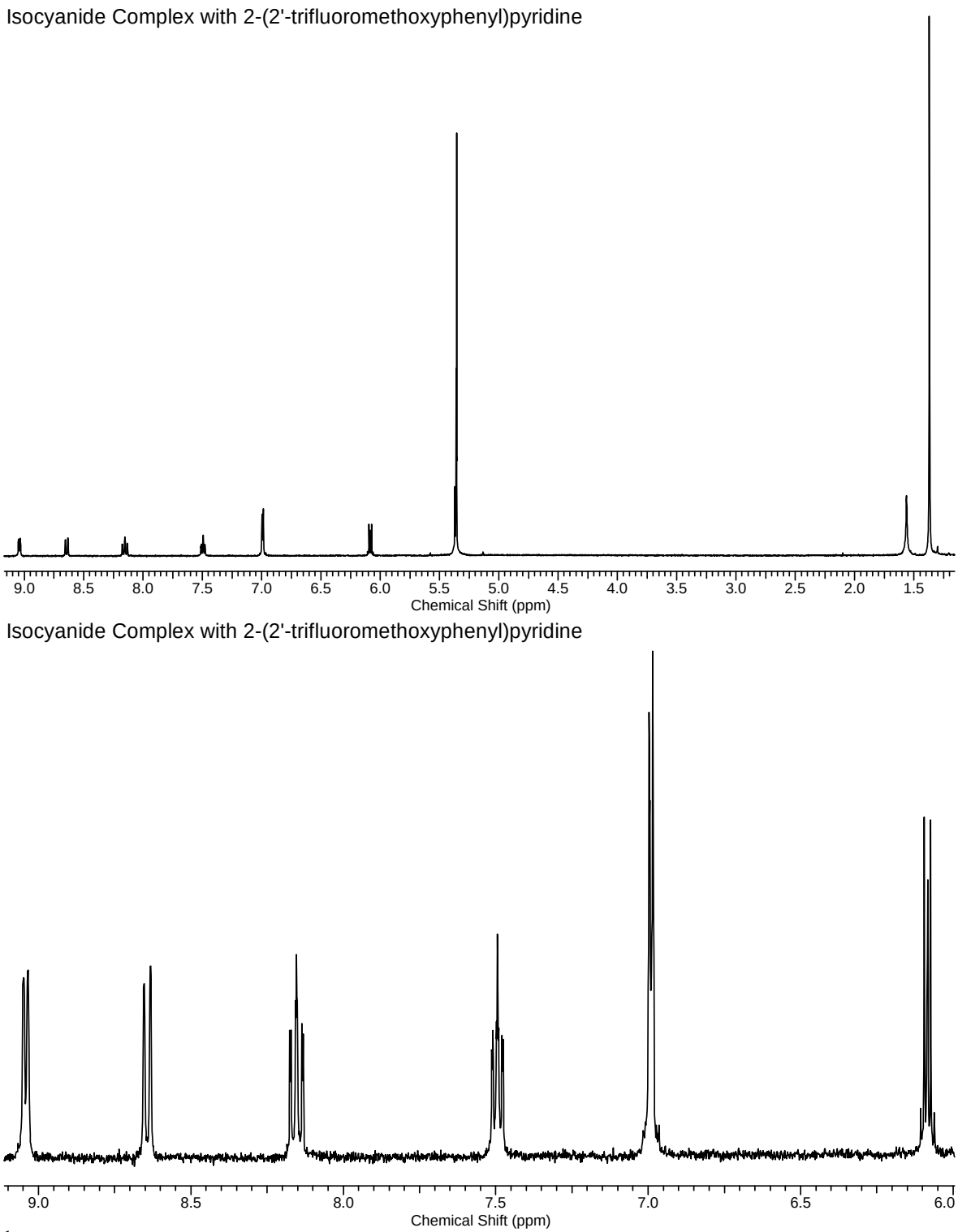

^{1}H NMR Spectrum of isocyanide complex with 2-(2′-trifluoromethoxyphenyl)pyridine in CD_2Cl_2 (top, complete; bottom, arom. H).

7-H. 2-(3′-Trifluoromethoxyphenyl)pyridine L8

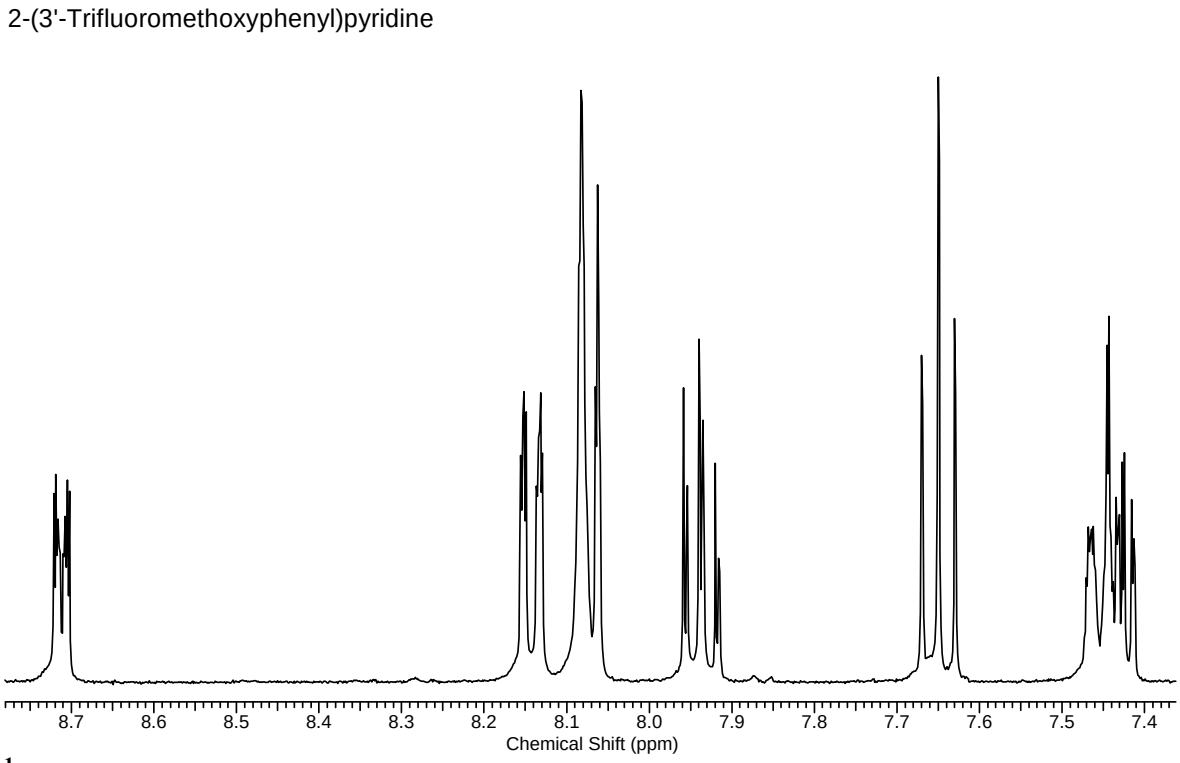

^{1}H NMR Spectrum of 2-(3′-trifluoromethoxyphenyl)pyridine in DMSO-d_6.

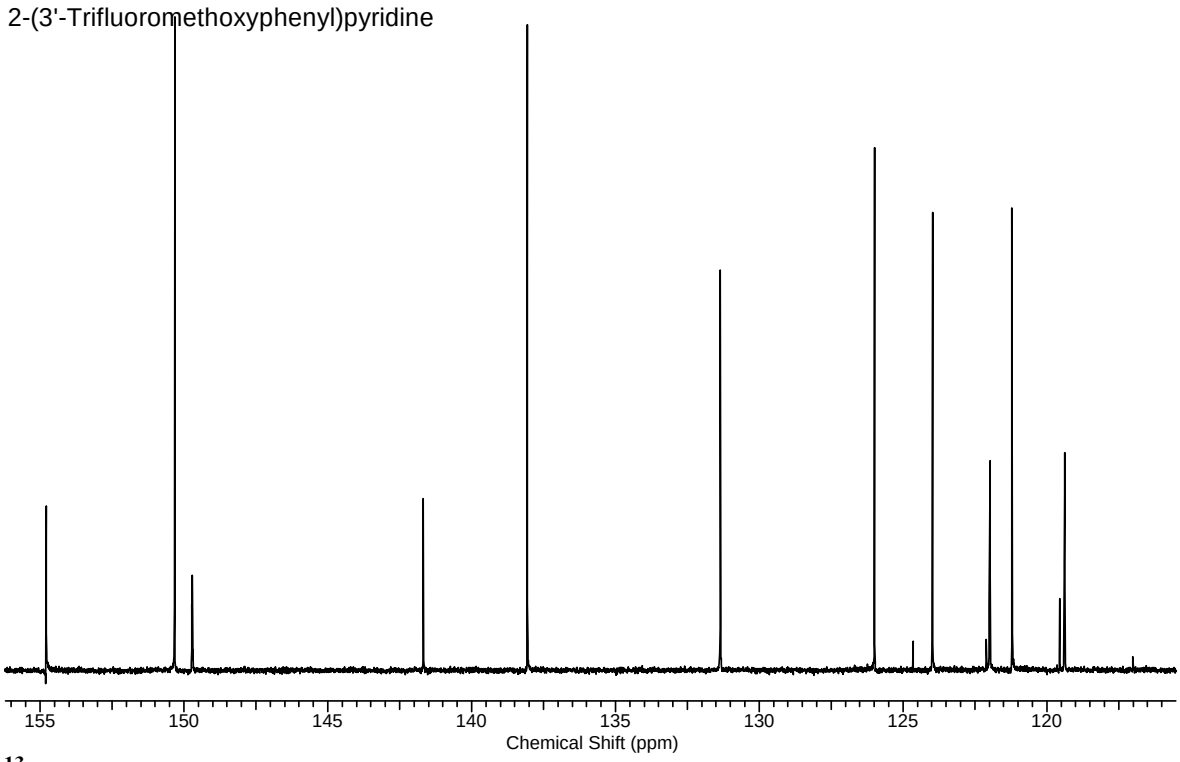

^{13}C NMR Spectrum of 2-(3′-trifluoromethoxyphenyl)pyridine in DMSO-d_6.

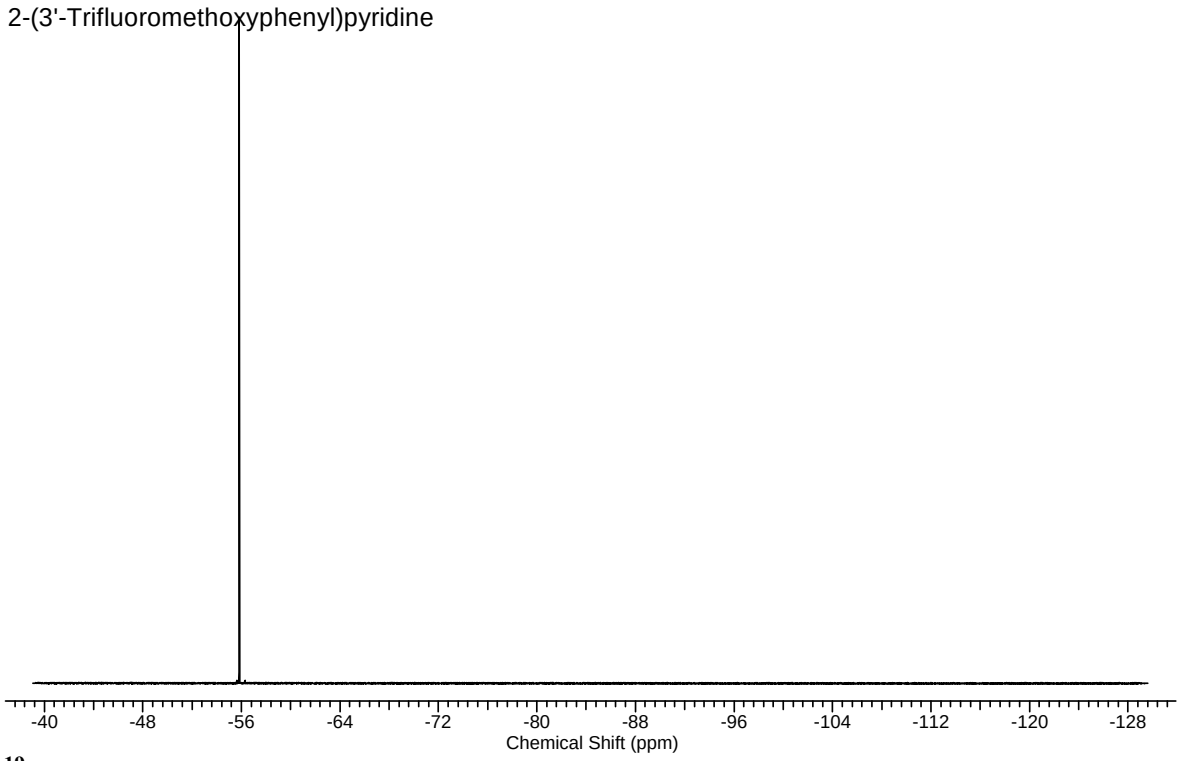

^{19}F NMR Spectrum of 2-(3′-trifluoromethoxyphenyl)pyridine in DMSO-d_6.

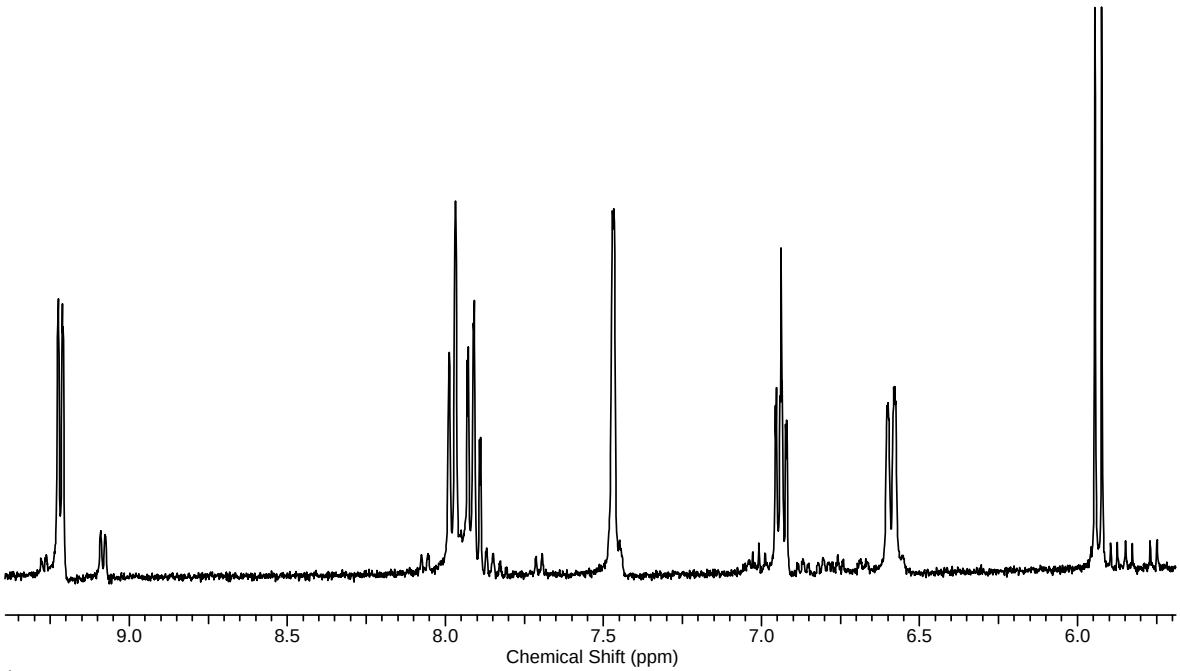

^{1}H NMR Spectrum (CD_2Cl_2) of the product of the reaction of $IrCl_3 \cdot 3H_2O$ with 2-(3′-trifluoromethoxyphenyl)pyridine.

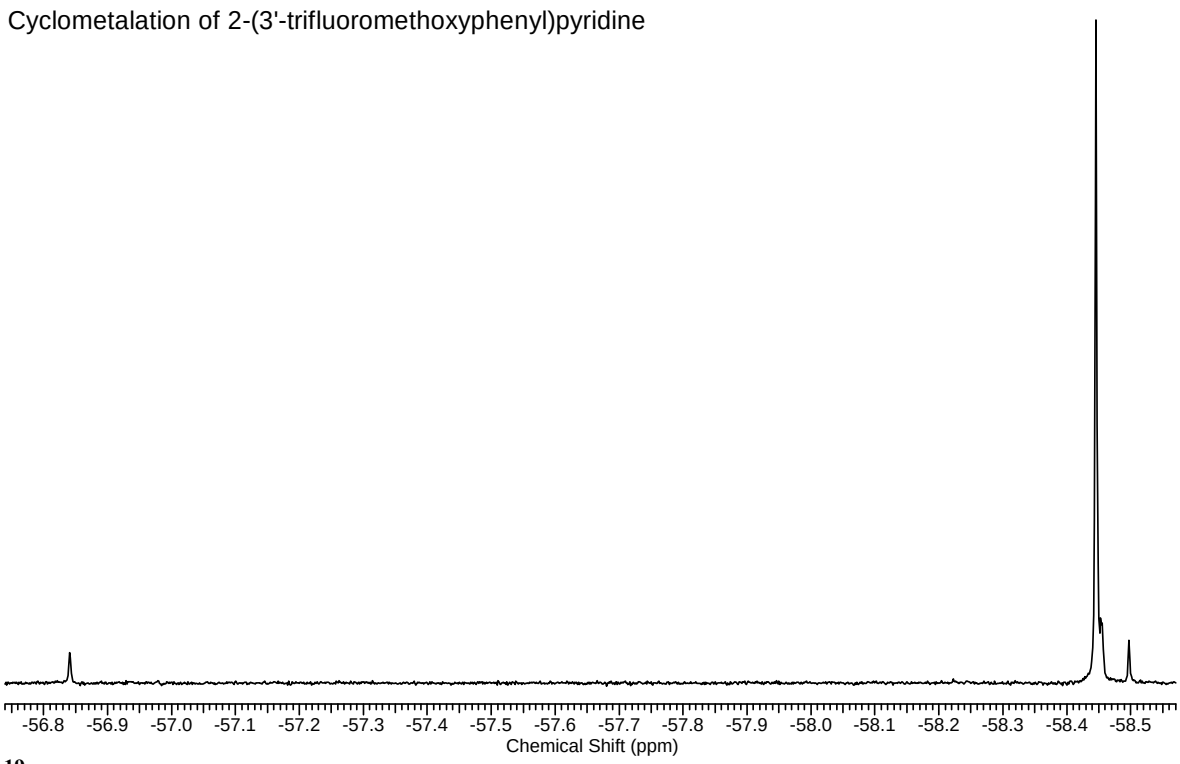

^{19}F NMR Spectrum (CD_2Cl_2) of the product of the reaction of $IrCl_3 \cdot 3H_2O$ with 2-(3′-trifluoromethoxyphenyl)pyridine.

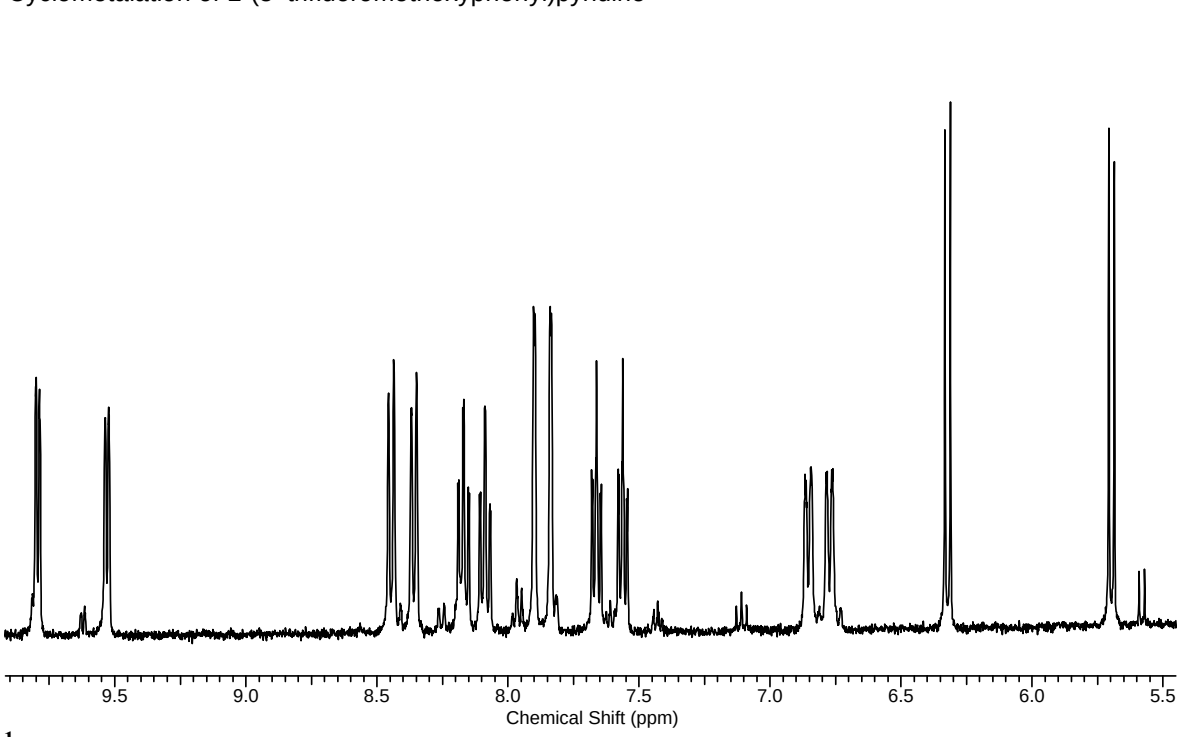

^{1}H NMR Spectrum (DMSO-d_6) of the product of the reaction of $IrCl_3 \cdot 3H_2O$ with 2-(3′-trifluoromethoxyphenyl)pyridine.

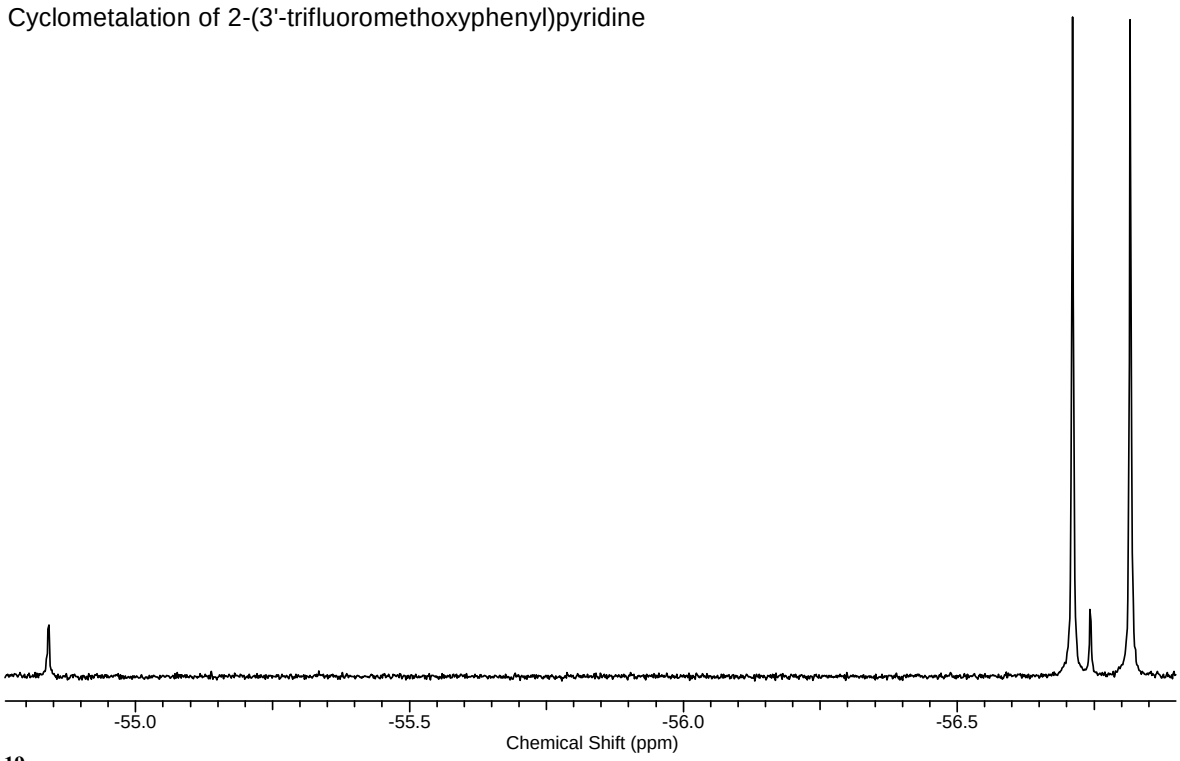

^{19}F NMR Spectrum (DMSO-d_6) of the product of the reaction of $IrCl_3 \cdot 3H_2O$ with 2-(3′-trifluoromethoxyphenyl)pyridine.